



**HAL**  
open science

## Lichen biomonitoring of airborne trace elements in the industrial-urbanized area of eastern algiers (Algeria)

Henia Saib, Amine Yekkour, Mohamed Toumi, Bouzid Guedioura, Mohamed Amine Benamar, Abdelhamid Zeghdaoui, Annabelle Austruy, David Bergé-Lefranc, Marcel Culcasi, Sylvia Pietri

### ► To cite this version:

Henia Saib, Amine Yekkour, Mohamed Toumi, Bouzid Guedioura, Mohamed Amine Benamar, et al.. Lichen biomonitoring of airborne trace elements in the industrial-urbanized area of eastern algiers (Algeria). *Atmospheric Pollution Research*, 2023, 14 (1), pp.101643. 10.1016/j.apr.2022.101643 . hal-03929895

**HAL Id: hal-03929895**

**<https://hal.science/hal-03929895>**

Submitted on 9 Jan 2023

**HAL** is a multi-disciplinary open access archive for the deposit and dissemination of scientific research documents, whether they are published or not. The documents may come from teaching and research institutions in France or abroad, or from public or private research centers.

L'archive ouverte pluridisciplinaire **HAL**, est destinée au dépôt et à la diffusion de documents scientifiques de niveau recherche, publiés ou non, émanant des établissements d'enseignement et de recherche français ou étrangers, des laboratoires publics ou privés.

# 1 Lichen biomonitoring of airborne trace elements in the industrial- 2 urbanized area of Eastern Algiers (Algeria)

3 Henia Saib<sup>1,2</sup>, Amine Yekkour<sup>3,4</sup>, Mohamed Toumi<sup>2,5</sup>, Bouzid Guedioura<sup>6</sup>,

4 Mohamed Amine Benamar<sup>7</sup>, Abdelhamid Zeghdaoui<sup>2</sup>, Annabelle Austruy<sup>8</sup>,

5 David Bergé-Lefranc<sup>1</sup>, Marcel Culcasi<sup>1</sup>, Sylvia Pietri<sup>1,8\*</sup>

6

7 <sup>1</sup>Aix Marseille Univ, CNRS, ICR, UMR 7273, SMBSO, Marseille, France

8 <sup>2</sup>Laboratory of Ethnobotany and Natural Substances - Department of Natural Sciences,

9 Ecole Normale Supérieure El-Ibrahimi Kouba, Algiers, Algeria

10 <sup>3</sup>Laboratory of Microbial Systems Biology, Ecole Normale Supérieure El-Ibrahimi Kouba, Algiers, Algeria

11 <sup>4</sup>National Institute of Agronomic Research of Algeria - Mehdi Boualem Station, Baraki, Algiers, Algeria

12 <sup>5</sup>Department of Natural and Life Sciences, Faculty of Sciences, University of Algiers, Algeria

13 <sup>6</sup>Reactor Division/CRND, Algeria

14 <sup>7</sup>Laboratory of Applied Physics, University Saad Dahleb, Blida, Algeria

15 <sup>8</sup>Institut Ecocitoyen pour la Connaissance des Pollutions, Fos-sur-Mer, France

16

## 17 Authors e-mail and ORCID addresses

18 [henia.saib@g.ens-kouba.dz](mailto:henia.saib@g.ens-kouba.dz) ; [amineyek@gmail.com](mailto:amineyek@gmail.com) ; [toumi\\_m2001@yahoo.fr](mailto:toumi_m2001@yahoo.fr) ; [algeryfx@gmail.com](mailto:algeryfx@gmail.com) ;

19 [benamardz64dz@gmail.com](mailto:benamardz64dz@gmail.com) ; [zeghdaouiens@hotmail.fr](mailto:zeghdaouiens@hotmail.fr) ; [annabelle.austruy@institut-ecocitoyen.fr](mailto:annabelle.austruy@institut-ecocitoyen.fr)

20 [david.BERGE-LEFRANC@univ-amu.fr](mailto:david.BERGE-LEFRANC@univ-amu.fr) ; [marcel.culcasi@cnrs.fr](mailto:marcel.culcasi@cnrs.fr) ; [sylvia.pietri@univ-amu.fr](mailto:sylvia.pietri@univ-amu.fr)

21

22 Henia Saib: <https://orcid.org/0000-0002-8009-3934>

23 Amine Yekkour: <https://orcid.org/0000-0003-3499-7374>

24 Mohamed Toumi: <https://orcid.org/0000-0003-485>

25 Annabelle Austruy: <https://orcid.org/0000-0002-7939-8036>

26 David Bergé-Lefranc : <https://orcid.org/0000-0002-2679-1571>

27 Marcel Culcasi: <https://orcid.org/0000-0002-7255-7591>

28 Sylvia Pietri: <https://orcid.org/0000-0002-9207-0780>

## 29 Corresponding author

30 Prof. Sylvia Pietri, E-mail: [sylvia.pietri@univ-amu.fr](mailto:sylvia.pietri@univ-amu.fr)

31 Aix Marseille Univ, CNRS, Institut de Chimie Radicalaire, UMR 7273, SMBSO

32 Centre Scientifique de Saint Jérôme, Service 522, Avenue Escadrille Normandie Niemen

33 F-13397 Marseille Cedex 20, France.

34

35 This paper is dedicated to the memory of Prof. Mohammed Rahali, our dear colleague and friend.

36

37 **Abstract**

38

39 This study established a comprehensive picture of airborne metal pollution in the industrial urbanized area of the  
40 East of Algiers (Algeria). Thalli of the epiphytic lichen *Pseudevernia furfuracea* were transplanted from a  
41 remote unpolluted forest (Theniet El-Had) to eighteen biomonitoring sites in the Rouiba–Reghaia region  
42 exhibiting contrasting anthropogenic activities, including the wooded Reghaia Nature Reserve. Thirty-three  
43 metals and rare earths, and Br in lichen thalli were determined after 3 months exposure by X-ray fluorescence  
44 and instrumental neutron activation analysis. All biomonitored element concentrations exhibited dramatic  
45 increases compared to the control region, and calculation of contamination factor index unveiled that Sb, Pb, Ti,  
46 V, Ce, La, Ga, Cr, Cs, Cu, and Cd had the highest contamination levels in almost all the study sites. The degree  
47 of ambient pollution was assessed using enrichment factor, pollution load index, cluster analysis, and principal  
48 components analysis. A multiple correspondence analysis showed Pb, Sb, and Ga to be highly enriched with  
49 heavy contamination in all study sites, even in the Reghaia Nature Reserve.

50

51 **Keywords.** Lichen biomonitoring; *Pseudevernia furfuracea*; Trace element pollution; Enrichment factor;  
52 Multivariate analysis.

53

54 **Abbreviations.** RNR, Reghaia nature reserve; RU, Reghaia urban area; IZ, Industrial zone of Rouiba–Reghaia;  
55 TH, Theniet El-Had region; CF, contamination factor; PLI, pollution load index; EF, enrichment factor; CA,  
56 Cluster analysis; PCA, principal component analysis; MCA, multiple correspondence analysis.

57

58

59 **1. Introduction**

60  
61 In the last decades airborne metal pollution has become a global environmental issue to be faced by public  
62 authorities due to increasing evidence of multiple adverse effects of trace elements on living organisms. For most  
63 metallic contaminants, the contribution of anthropogenic inputs has far outpaced that of natural sources and there  
64 is evidence that airborne particulate matter-bound species, including metals, accumulate in the human body to  
65 trigger chronic pathologies such as neurological degenerative processes, multiple sclerosis or muscular  
66 dystrophy (Rehman et al., 2018), and lung cancer (Swanton et al., 2022). Biosensors that have been extensively  
67 used to assess air pollution locally include lichens (Boonpeng et al., 2017; Demková et al., 2017; Dron et al.,  
68 2021), mosses (Zechmeister et al., 2005; Vuković et al., 2016;), plant leaves or tree rings (Austruy et al., 2019).

69 Lichens are perennial organisms devoid of any root system or other absorptive organs, protective cuticles,  
70 and filtration mechanisms, which maintain a uniform morphology over time with a high surface/volume ratio.  
71 These properties confer to lichens an exceptional ability to easily accumulate airborne pollutants, particularly  
72 metals, at levels exceeding their physiological needs to some extent (Conti and Cechitti, 2001; Sorbo et al., 2008;  
73 Osyczka et al., 2018). Consequently, lichens are commonly used in air quality studies and heavy metal  
74 biomonitoring through measurement of pollutants levels accumulating in their thalli in the long term, in the area  
75 where these species grow (Bari et al., 2001; Aslan et al., 2013; Paoli et al., 2015; Ratier et al., 2018; Massimi et  
76 al., 2019).

77 However, such studies are hardly realizable using endogenous lichens under conditions of unusual dramatic  
78 pollution bursts or extended periods at high levels that outperform their homeostatic efficiencies and reduce their  
79 abundance (Agnan et al., 2017). To keep the advantage of using lichen pollution biosensors in conditions and/or  
80 areas where these species are scarce or absent, alternative transplant techniques have been proposed (Basile et  
81 al., 2008; Nannoni et al., 2015; Paoli et al., 2015). Globally, this involves relocating thalli from an area deemed  
82 as uncontaminated to remote sites under study for a short period of time, and it has been shown such lichens  
83 transplants to be good quantitative probes of atmospheric heavy metals distribution (Boamponsem et al., 2010,  
84 2017; Incerti et al., 2017; Kodnik et al., 2017; Zhao et al., 2019) and powerful witnesses of the effectiveness of  
85 anti-pollution regulations (Lucadamo et al., 2022).

86 In Algeria, lichen-based biosensing of trace element contamination, as well as an accurate knowledge of  
87 atmospheric metallic pollutants concentrations in the main industrial and urban areas are still scarce. Previous  
88 lichen studies have documented only a limited number of airborne metal elements such as Pb in Algiers and

89 Annaba (Rahali, 2002; Semadi, 1993), Pb and Zn in Tiaret (Maatoug et al., 2010) or a group of 10 heavy metals  
90 in the Bordj Bou Arreridj area (Adjiri et al., 2018).

91 The aim of this study was to present the first detailed inventory of atmospheric heavy metal contamination in  
92 the Rouiba–Reghaia region, one of the largest, very active, and populated urban-industrial areas of Algeria (East  
93 of Algiers, Fig 1A) where autochthonous lichens are yet poorly available. The macro lichen *Pseudevernia*  
94 *furfuracea* (L.) Zopf v. *furfuracea* was used as a transplanted biomonitor for a large set of 33 rare earths and  
95 metal elements accumulating during a three months exposure period in eighteen sites, including a wooded nature  
96 reserve. Lichens, which were presumably subjected to low, medium or high levels of atmospheric pollution,  
97 were compared to samples transplanted in the unpolluted Theniet El-Had National Park Forest control region.  
98 Further, two approaches were performed to discriminate between anthropogenic (industry, traffic) and natural  
99 (crustal materials, marine aerosols) sources of trace metals, i.e., by determining the enrichment factor for each  
100 individual element, and by performing multivariate statistical techniques.

101 Altogether, the data acquired here enabled: (i) the build-up of a database of atmospheric pollution in three  
102 contrasting environments, i.e., rural, urban, and industrial sites, and (ii) to validate the usefulness of  
103 *Pseudevernia furfuracea* lichen as an enhanced pollution biomonitoring species for an array of airborne metals.

104

## 105 **2. Materials and methods**

106

### 107 *2.1. Study area, monitoring sites, and meteorological conditions*

108

109 The studied region of Rouiba–Reghaia, located at 30 km from the East of Algiers, represents a suburban area  
110 where agricultural, industrial activities, and road traffic are preponderant and have constantly increased over the  
111 past 30 years. In this surface area of about 2,600 hectares, eighteen random sampling stations were established in  
112 order to account for the contribution of each of the main local metal emission sources, including the intense  
113 railway and road traffics, and were located along a presumed increasing pollution gradient (Fig 1B). Eighteen  
114 monitoring stations were designed as follows: (1) the Reghaia Nature Reserve (RNR; 3 sampling sites) according  
115 to the Ramsar Convention 2003, located in a wooded area including a lake, (2) the Reghaia Urban area (RU; 3  
116 sampling sites), a densely populated zone (estimated at 2,700 inhabitants per km<sup>2</sup>) with an important  
117 demographic growth, and subjected to the influence of local emissions, agriculture, railway and road traffic of  
118 the city, and (3) the industrial Rouiba–Reghaia zone (IZ1–4; 12 sampling sites, see Fig. 1B–C), one of the  
119 largest industrial areas in the country (1,000 hectares) with 250 mechanical, metallurgical, chemical and food

120 processing units implanted along the railway. Lichens were then submitted to various sources of pollution,  
121 notably the high density of road traffic, the influence of agricultural and multiple industrial pollution sources  
122 from Reghaia, as well as the proximity of the Dar El Beïda airport (Fig. 1B). Geographical coordinates of each  
123 site are reported in the Supplementary materials (Table S1). The locations of industrial facilities are often  
124 intertwined with residential neighborhoods. On the basis of census data in Wilaya–Algiers, the city had a  
125 population of 155,710 inhabitants in 2015. Moreover, this urban-industrial region also includes the East–West  
126 highway (A1), three main national roads (NR5, NR11, and NR24), and the Algiers–Blida railway (Fig. 1B).

127 Globally, the region is characterized by a Mediterranean climate, with a mild winter with heavy rainfall and a  
128 hot and dry summer with an arid period extending from the midst of May until the end of September. According  
129 to the data from the local meteorological station of Dar El Beïda (2008–2018), the annual average of  
130 precipitation is 660 mm, the temperature ranges 12.0–24.3 °C with an average of 18.1 °C and a relative humidity  
131 of 74%. The prevailing frequent winds are from the North and North–East, with an average wind speed of 10.4  
132 m/s. The station of Algiers is located at the inferior sub-humid bioclimatic stage of the temperate winter.

133 Three additional monitoring stations distant of at least 10 km each other were established in the Theniet El-  
134 Had National Park Forest (TH). This area (700 m above sea level), located 200 km from the Rouïba–Reghaïa  
135 area in northwestern Algeria (Fig. 1A), was taken as a relatively unpolluted control site in the study. With a  
136 surface area of 3,500 hectares and a mountain peak standing at 1,787 m (Ras El-Braret), the TH consists of vast  
137 forests of Atlas cedars (*Cedrus atlantica*) with diverse flora and fauna of value.

138

## 139 2.2. *Lichen sampling and transplantation procedures*

140 The fruticose epiphytic macro lichen *Pseudevernia furfuracea* (L.) Zopf v. *furfuracea* was chosen since it  
141 is largely employed in biomonitoring studies with transplants (Sorbo et al., 2008; Malaspina et al., 2014). Thalli  
142 of seemingly healthy lichens from the clean TH area were carefully collected with adhering bark substrate from  
143 mature *Cedrus atlantica* trees having similar sizes, at 1.5–2.5 m above the ground and all around each tree to  
144 minimize contamination by soil and any influence of prevailing winds. Samples, excluding over and densely  
145 isidiate thalli, were transferred to the laboratory in individual polyethylene bags, and then carefully cleaned from  
146 foreign materials and debris. The thalli were manipulated as promptly as possible to avoid any source of stress.  
147 Before transplantation, samples vitality was checked by analyzing their photosynthetic efficiency by measuring  
148 chlorophyll fluorescence (Garty et al., 2000).

149 One day after sample collection, about 150 thalli were transplanted to the 21 monitoring sites according to  
150 the procedure of Cuny et al. (2001). Thalli were arranged on 20 × 40 cm wooden boards (3 thalli per board,  
151 technical replicates) and three of these boards were installed at each studied site on three trees separated by at  
152 least 5 m each other (triplicates), as illustrated in Figure S1 (Supplementary materials). Once transplanted, the  
153 lichens were kept in the monitoring sites for an optimal duration of 3 months for pollution measurements (Fрати  
154 et al., 2005; Gallo et al., 2014; Lucadamo et al., 2016), in winter period (January–April), an ideal season for  
155 lichen growth in Algeria, before being collected for trace element analysis.

156

### 157 2.3. *Sample preparation and trace element analysis*

158

159 Following collection experimental lichens were carefully cleaned using plastic tweezers to remove dusts and  
160 residue, and then placed in small Pyrex Petri dishes without prior washing (Saiki et al., 1997, Boonpeng et al.,  
161 2017). Afterwards, they were oven-dried at 80 °C for at least 48 h, crushed and homogenized in a grinding mill,  
162 and sieved through a 2-mm pore size mesh. The recovered powder was stored at ambient temperature before  
163 analyses. A diversity of methods are available for elemental analysis of lichens, including atomic absorption  
164 spectroscopy, inductively coupled plasma-mass spectroscopy, INAA, and XRF. Here, INAA (see 2.3.1) and  
165 XRF (see 2.3.2) were selected because they are both powerful non-destructive multielemental techniques  
166 (Herrero Fernández et al., 2015; Pantelica et al., 2016).

167

#### 168 2.3.1. *Instrumental neutron activation analysis (INAA)*

169 INAA, one of the most sensitive and accurate techniques for trace elements determination, was applied for  
170 quantifying one halogen (Br), and a series of heavy metals and rare earths including Al, In, Mn, Ti, V, As, Ba,  
171 Co, Cu, Cr, Cs, Hf, Fe, Ga, La, Ce, Nd, Sm, Eu, Tb, Yb, Lu, Hg, Rb, Sb, Sc, Se, Th, U, and Zn. Irradiation  
172 procedures were carried out using the NUR research reactor at the Draria Nuclear Research Center in Algiers  
173 (Algeria). Three sub-samples, each containing 100 mg of lichen powder, standards, and blanks, were weighed,  
174 heat-sealed in polyethylene bags and packed in high-purity (99.99%) aluminum foil for irradiation. For the  
175 determination of short-lived radionuclides (i.e., Al, In, Mn, Ti, V), lichen samples, standards, and blanks were  
176 simultaneously irradiated for 200 s in the pneumatic transfer system under a thermal neutron fluence rate of 5.4  
177  $\times 10^{12}$  cm<sup>-2</sup>. s<sup>-1</sup>. For the analysis of longer-lived radioisotopes (i.e., As, Ba, Br, Co, Cu, Cr, Cs, Hf, Fe, Ga, La, Ce,  
178 Nd, Sm, Eu, Tb, Yb, Lu, Hg, Rb, Sb, Sc, Se, Th, U, and Zn), the irradiation scheme involved irradiation for 18 h  
179 under a neutron fluence rate of  $2.7 \times 10^{13}$  cm<sup>-2</sup>.s<sup>-1</sup> (Guedioura et al., 2014; Bouhila et al., 2015). For short

180 irradiated samples, gamma-ray counting was carried out after a decay time of 300 s while for long irradiated  
181 samples two successive countings were performed after a decay period of 1 day and 7–10 days, respectively.  
182 Gamma-ray counting was carried out using a hyper-pure germanium (HPGe) detector (Mirion Technologies  
183 (Canberra), Montigny-le-Bretonneux, France). HPGe detector main characteristics, spectral processing,  
184 calculations and quality controls using Tulip sample (IPE-175) and epiphytic lichen material (IAEA-336) as  
185 certified standards are given in the Supplementary materials.

186 Concentrations were expressed on a dry weight (dw) basis. Samples were analyzed in duplicate and the  
187 instrumental limits of detection were found as follows (in  $\mu\text{g}\cdot\text{g}^{-1}$  dw): Al, 84.6; As, 0.19; Ba, 0.61; Br, 0.28; Co,  
188 0.04; Cu, 0.1; Cr, 0.08; Cs, 0.17; In, 0.05; Fe, 7.33; Ga, 0.61; Hf, 0.09; La, 0.1; Ce, 0.14; Nd, 0.90; Sm, 0.01; Eu,  
189 0.01; Tb, 0.01; Yb, 0.04; Lu, 0.005; Mn, 12.9; Hg, 0.04; Rb, 0.1; Sb, 0.06; Sc, 0.002; Se, 0.1; Ti, 0.5; V, 0.62;  
190 Th, 0.10; U, 0.01, and Zn, 1.31.

191

### 192 2.3.2. *X-ray fluorescence spectroscopy (XRF)*

193 X-ray fluorescence spectroscopy analysis, an accurate technique for quantifying environmentally important  
194 heavy metals such as Cd and Pb in lichens, was performed at the Applied Physics Laboratory of Blida University  
195 (Algeria). An X-ray fluorescence spectrometer (Malvern Panalytical Epsilon 3XLE, Palaiseau, France), with  
196 silicon drift detectors (SDD with Peltier effect, resolution 132.6 keV for  $K\alpha$ -Mn X-ray) and X-ray tube  
197 excitation (primary target Ag, 50 kV; Malvern Panalytical) was used according to Rekik et al (2016). X-ray  
198 spectra were identified using the Epsilon 3 XL software (version 1.3.A. (8.24), 2014). The yields of the  
199 characteristic X-ray peaks ( $K\alpha$ -Cd,  $L\alpha$ -Pb) were quantified after adjustment and subtraction of the background  
200 noise. Elements contents were determined by the Omnia process with various filters (Cu-500, Al-200, Al-50,  
201 Ti, Ag) and without filters and compared to IPE175 and IAEA-336 standards irradiated under the same  
202 conditions.

203 For INAA and XRF analysis the results of the quality controls on certified materials are given in Tables S2  
204 and S3 (Supplementary materials).

205

### 206 2.4. *Calculation of environmental indexes of pollution*

207

208 To estimate the air pollution level within the study area, calculations of several environmental indexes of air  
209 pollution were performed for each element and monitoring site, such as contamination and enrichment factors,  
210 and pollution load index.



211

212 *2.4.1. Contamination factor*

213 The contamination factor (CF) was calculated to estimate the atmospheric contamination level of each  
214 element in each monitoring site as follows:

215 
$$CF = C_s/C_c \tag{1}$$

216 where  $C_s$  is the mean concentration of each element in the transplanted lichens at a given monitoring site and  
217  $C_c$  is the corresponding average concentration at the TH control site (triplicates of the values obtained in 3  
218 independent locations in TH).

219

220 Ranges of CFs were categorized into the following four contamination classes according to Boamponsem et  
221 al. (2010), as [CF range, contamination]: [ $< 1.2$ , none]; [ $1.2-2$ , light]; [ $2-3$ , medium], and [ $\geq 3$ , heavy]. For each  
222 element at the TH control site, a CF value of 1 is taken as the background level.

223

224 *2.4.2. Pollution load index*

225 The pollution load index (PLI) was calculated as follows:

226 
$$PLI = (CF_1 \times CF_2 \times CF_3 \times CF_4 \times \dots \times CF_n)^{1/n} \tag{2}$$

227 where CF is the contamination factor of each selected element and  $n$  refers to the number of studied  
228 elements.

229 According to Boonpeng et al. (2017) a PLI value  $< 0.9$  indicates an unpolluted area, whereas PLI ranges  $> 1$   
230 were assigned to the following pollution levels:  $1.1 < PLI < 1.5$ , low;  $1.5 \leq PLI < 2.0$ , moderate;  $2.0 \leq PLI < 2.5$ ,  
231 high;  $PLI \geq 2.5$ , very high.

232 For each element recovered at the TH control site a background PLI value of 1 was taken.

233

234 *2.4.3. Enrichment factor*

235 The enrichment factor (EF), commonly used as an index to distinguish whether trace elements recovered in  
236 lichen samples may originate from either natural or anthropogenic sources (Pacheco and Freitas, 2009), was  
237 calculated as follows:

238 
$$EF = (C_e/C_R)_{\text{Sample}} / (C_e/C_R)_{\text{Crust}} \tag{3}$$

239 where  $C_e$  is the concentration of the studied element and  $C_R$  is the concentration of the reference.

240

241 The  $(C_e/C_R)_{\text{Sample}}$  ratio was calculated using concentrations in lichen samples and the  $(C_e/C_R)_{\text{Crust}}$  ratio was  
242 calculated as the average elemental richness in the Earth's crust, using the CRC upper continental crust manual  
243 (Lide, 2005). Then, EF was calculated for each element, with Al taken as a reference, since it rarely enters the

244 atmospheric aerosols from anthropogenic sources (Reiman and Decarital, 2000; Kłos et al., 2011; Agnan et al.,  
245 2015; Wu et al, 2020). According to Xiong et al. (2017), an EF based classification of elements was established  
246 as follows: [class; EF range; grade]: [class 1;  $\leq 1$ , rare], soil and crust sources; [class 2; 2–10, mild], natural and  
247 anthropogenic; [class 3; 10–100, moderate], only anthropogenic); [class 4; 100–1000, high], artificial, and [class  
248 5;  $> 1000$ , extreme], artificial.

249

## 250 2.5. Statistics and data analysis

251

252 Data were analyzed by several statistical methods using FactoMineR R package 3.5.2 (Lê et al., 2008).  
253 Differences between element concentrations at TH control vs. each monitoring site were analyzed by a one-way  
254 analysis of variance (ANOVA) and Dunnett's post-hoc test for mean comparison. Difference were considered  
255 significant when  $P < 0.05$ .

256 In order to focus on lichen trace elements concentration at each sampling site and to estimate the pollution  
257 level, a data matrix of mean concentrations was constructed. Standardized data were computed to account for  
258 scale differences as documented earlier (Bozkurt et al., 2017; Incerti et al., 2017). The matrix was submitted to  
259 cluster analysis (CA) using Euclidean distance and complete linkage algorithm as previously described (Brunialti  
260 and Frati, 2007; Demiray et al., 2012) and principal component analysis (PCA). For interpretation purpose PLI  
261 was included in the PCA as supplementary variable (i.e., plotted in the multivariate space, but not used to  
262 calculate the principal components) as proposed (Legendre and Legendre, 1998).

263 To estimate the pollution impact of selected elements over sites a multiple correspondence analysis (MCA)  
264 was performed by considering the experimental CF and EF data in a complete disjunctive matrix as a binary  
265 'dummy variable' assuming values 1 or 0 according to their corresponding categorical class indicator (Greenacre,  
266 2017) given in 1.4.1 (for CF) and 1.4.3 (for EF).

## 267 3. Results

268

269 One of the main interests of this study was to determine the spatial distribution of an array of 33 relevant airborne  
270 contaminants accumulated in thalli of *P. furfuracea* transplants in the area of Rouiba–Reghaia, as a consequence  
271 of anthropic pollution sources such as industrial activities, urbanization, road traffic, and agriculture. On the  
272 basis of the set of the measured trace elements content, a preliminar cluster analysis (CA) which aimed at  
273 splitting the twenty-one sampling sites into a number of different reasonable homogeneous groups, such that  
274 similar sites are placed in the same groups, was undertaken to judge the global inter-sites differences. As shown

275 in Fig 2A, in addition to the TH control area, six homogeneous groups (RU, RNR, IZ1–4), were obtained by  
276 grouping the means from the 18 sampling sites having the same typology over the studied zone. Accordingly, for  
277 the further analysis of the study data, each group was considered as a homogeneous “studied area” defined by a  
278 mean content for each trace element.

279

### 280 3.1. Spatial variations in the accumulation of trace elements in lichen transplants

281 Table 1 shows the mean concentrations of 33 trace elements in transplanted lichens after a 3-month exposure  
282 in the six monitoring urban–industrial sites defined above, in comparison with background values from native *in*  
283 *situ* lichens transplanted in the unpolluted TH control site. Among the elements monitored in the industrial sites  
284 IZ1–4, seventeen of the metals and rare earth elements, including Cd, Cu, Cs, Ga, Sb, Pb, V, and Ti and, in a  
285 lesser extent, Cr, Al and Zn, were found at concentrations up to 890-fold higher than those found at TH ( $P <$   
286  $0.05$  or less). For most of the studied elements concentrations peaked in the IZ4 area, located in the vicinity of  
287 mixed anthropogenic pollution sources including a foundry, several factories, roads and railway traffic (Fig. 1C).  
288 While IZ4 region exhibited the most elevated concentrations of Al, Cd, Cu, Ga, Cs, La, Cr, Sb, Pb, V, Ce, Hf,  
289 Sm, Lu, Eu, Yb, Th, and U other elements including Mn, Ti, Zn, Br, and Co were found noticeably higher at IZ2  
290 site. However, among the assayed metals the highest concentrations of Fe, Tb, and Sc were found at IZ1 site,  
291 while Nd and In levels culminated locally in lichens transplanted at IZ2,3 sites.

292 In transplants from the urban area RU, eighteen elements exhibited high concentrations, especially Ti, Cu,  
293 Rb, and Ga whose levels were found 190–350-fold higher than in control TH site. Strikingly, fifteen elements  
294 (especially Ti, Ga, Cu, and Cd) were found at high concentrations (30–120 fold higher than TH) in the RNR  
295 (Table 1).

296

### 297 3.2. Contamination factor and pollution load index

298 To assess the individual rates of trace elements accumulation, about 200 CFs were calculated from the  
299 concentrations of Table 1 and the results are listed in Table 2. Across the whole Rouiba–Reghaia region, CFs  
300 dramatically varied among assayed elements and sampling sites, being as low as 0.11 for Se at IZ1 while  
301 peaking at 893 for Ti at IZ2. Thus, regardless of the sampling zone and according to the classification of  
302 Boamponsem et al. (2010) (see 2.4.1), 52% of the studied areas were identified as severely contaminated, 17%  
303 exhibited a medium contamination, 14% were weakly polluted, and in only 17% of selected areas contamination  
304 was found negligible.

307 Next, PLIs were calculated from the CFs for further understanding the implication of air pollutants deposition  
308 and its repartition between the six selected areas. According to the ranking of 2.4.2 all regions exhibited very  
309 high PLIs, ranging from 2.87 at the RNR site to 7.08 at the IZ4 industrial site (Table 2).

310 A combined examination of CF and PLI values revealed that, despite it is very distant from the main sources  
311 of anthropogenic emissions, the RNR area was found strongly polluted by twelve elements, including several  
312 metals (Cd, Cu, Cr, Ga, Hg, Ti, V) with only a few elements being recovered at non contaminant levels (i.e., Ba,  
313 Fe, Yb, Rb, and Se). Moreover, Br and Hg sampled there afforded the highest CFs as compared to all other  
314 sampling sites. The fact that, in the RU zone adjacent to RNR CFs for most elements, particularly for Cu, La, Ce,  
315 Tb, Sb, Yb, Rb, and Ti, were found increased, (e.g., being 7- and 140-fold more elevated for Cu and Rb,  
316 respectively) may explain why RU showed a higher PLI value (Table 2).

317 As expected, the four IZ industrial areas resulted in the most elevated PLIs in relation with dramatic increases  
318 in the CFs. Hence, the IZ4 site was found the most impacted by air pollution, having  $CF \gg 3$  for 21 elements and  
319 a PLI  $\sim 7$  and in this area the lichen contents increases were (times): Rb (123), Sb (63), Ti (4), V (2), Cu (10), Cr  
320 2), Cd (7), and La (33) as compared to RNR. Contrary to these strong metal pollutants, the low CFs for Ba and  
321 Se recorded at all sites suggested these elements were insignificant pollutants in the whole studied region.

### 322 323 3.3. Enrichment factor calculations

324 According to the classification of Xiong et al. (2017), As, Cd, Cu, In, Hf, La, Hg, Zn, Br, Se, Pb, and Ga  
325 were moderately to highly enriched in the vast majority of study sites (Table 2), showing their main  
326 anthropogenic origin. Noteworthy, highly elevated EFs  $> 350$  were found for Sb in RU and IZ sites, peaking at  
327 4167 at IZ3. Regarding EFs even the RNR zone was highly impacted, e.g., by Ga Sb, Se, and Pb.

329 EFs  $\leq 1$  were recorded for Ba and Cr over the whole studied zones, indicating they may originate mainly  
330 from soil and crust sources. The class 1 and 2 distribution of EFs for Al, Sc, Rb, Fe, Co, Nd, Sm, Tb, Lu, Sc, Ti,  
331 V, Th, U, Ce, Eu, Yb, and Mn suggests that these elements may originate from both natural and artificial  
332 sources.

### 333 334 3.4. Multivariate analysis

335 Cluster analysis, used to distinguish between the most polluted sites, allowed to differentiate IZ4 (Cluster 3)  
336 from the other IZ1–3 sites (Cluster 2) which showed a similar lower pollution exposure level (Fig. 2B).  
337 Unexpectedly, the RU and RNR sites could be grouped into the same less exposed Cluster 1, yet exhibiting a  
338

339 statistically higher contamination than the TH control zone (Cluster 4). This distinction of TH as an outgroup  
340 confirmed the consistency of the choice of the Theniet El-Had National Park as a non polluted site. A further CA  
341 analysis over all studied sites allowed splitting the pollutants into the most (Al, Fe, Mn, Pb, and Zn; Cluster I),  
342 average (e.g., Ti, Cu, and Sb; Cluster II), and less (Cluster III) abundant elements (Fig. 2C).

343 In order to determine the influence of each element in the classification of the sampling sites, a PCA was  
344 performed on the basis of element contents recorded at each site. Despite the narrowness of the regional area of  
345 interest limited the number of samples sites vs. the number of assayed elements, the reliability of the PCA  
346 remains acceptable enough for a preliminary (Filzmoser and Reimann, 2002). As illustrated in Fig. 3A, the first  
347 two principal components PC1 and PC2 accounted for 75% of the total variance recorded in the trace element  
348 data set. The PC1 component accounted for 59% of the total variance and was positively correlated with almost  
349 all measured elements, except Se which appears negatively correlated while Ba, As, and Br are not correlated.  
350 Furthermore, the PLIs, which were plotted as a supplementary variable, were also positively correlated with PC1  
351 (Fig. 3B). Globally, Figure 3 allowed ranking the global extent of pollution among sites as follows: IZ4 > IZ2 >  
352 IZ1 > IZ3 > RU ≥ RNR, a result in accordance with cluster analysis of Figure 2. Moreover, elements of Cluster I  
353 (except Pb) were negatively correlated with PC2, but almost all elements belonging to Clusters II and III were  
354 correlated with PC1. In addition to Pb, Cd, Cu, Cr, Ga, Hf, La, Ce, Sm, Hg, Sb, Ti, V, Th, and U (in Clusters II  
355 and III; Fig. 2B) were found to account for ~70% of the PC1 computation (Table S4; Supplementary materials),  
356 suggesting they are the main air pollutants in the studied area.

357 The results of MCA are shown in Figure 4, evidencing that the first two plots (MC1 vs. MC2) accounted for  
358 95% of the total measured correspondence. Among the variables, CF2–EF1; CF3–EF2; CF4–EF3 and to a lesser  
359 extent CF4–EF4, and CF4–EF5 appeared clearly associated. Trace elements gathered in Groups 12, 15, and 17  
360 expressed both the highest CFs and EFs (CF class 4 and EF classes 3–5). According to these Groups, the most  
361 accumulated and enriched elements in the industrial sites, especially in IZ2,4, were Sb, Zn, Cu, and La, whereas  
362 Pb, Ga, and Cd mainly accumulated in both urban and industrial sites.

363

## 364 **4. Discussion**

365

### 366 *4.1. Bioaccumulation of trace elements*

367

368 It was not unexpected that heavy metals and rare earths concentrations in *Pseudevernia furfuracea* lichen  
369 transplants are significantly higher in all selected urban-industrial sites of Rouiba–Reghaia region relative to the

370 Reghaia Nature Reserve and the Theniet El-Had control site. In this latter regard, background elements  
371 concentrations found at the TH site are plausible control levels (Bergamaschi et al., 2004; Ancora et al., 2021) in  
372 agreement with the literature values obtained in unpolluted sites worldwide listed in Table S5 (Freitas et al.,  
373 1993; Adamo et al., 2003; Culicov and Yurukova, 2006; Malaspina et al., 2014; Pantelica et al., 2016). Indeed,  
374 lichen biomonitoring studies, including the present investigation, have identified Al, Fe, and, in a lesser extent,  
375 Mn and Zn, as the major contributors to the contemporary background atmospheric burden.

376 The amounts of recovered elements over a sampling area depend on several factors, including the nature, the  
377 distance, and the strength of the pollution sources (Bozkurt, 2017), the lichen species and its bioaccumulation  
378 ability, and the accurate analytical methods used. Table 3 allows comparison of the average concentrations of  
379 airborne elements for the whole Rouiba–Reghaia region with comparable biomonitoring surveys in urbanized  
380 areas of Bosnia Herzegovina (Humerovic et al., 2015), The Netherlands (de Bruin, 1990), Brazil (Saiki et al.,  
381 1997), China (Zhao et al., 2019), France (Ratier et al., 2018), and Italy (Adamo et al., 2003; Frati et al., 2005;  
382 Malaspina et al., 2014). Besides the fact that still Al and Fe remained the most dominant pollutants, followed by  
383 significant contributions of Cu, Pb, Mn, Ti, and Zn, the present study also pinpointed at Pb, Cd, Sb, and Cu as  
384 unusually strong atmospheric pollutants as compared to other regions worldwide, and at Ba, Cr, Sc, Se and U as  
385 relatively low contaminants. Strikingly, La levels were significantly higher in the Rouiba–Reghaia region (2- to  
386 25-fold; see Table 3), a worrisome concern owing to the emergence of pollution by rare earths (Zhao et al.,  
387 2019).

#### 388 4.2. *Sites classification* 389

390 Perhaps the most important result of this study is that, although the RNR and RU areas have similar  
391 lithological features and their average distance from the strongly polluted industrial IZ4 site is only 13 km and  
392 20 km, respectively, they belong to the same Cluster 1 based on CA (Fig. 2B) and high PLIs (Table 2), yet RNR  
393 retained the lowest overall contamination level (Table 1). These data can help advocate for saving urban forests  
394 and/or enhancing large green spaces installation for providing barriers against airborne pollutants that are  
395 intensively spreading from the industrial zones to the rural and urban areas. In this regard, recent approaches  
396 were proposed for modeling the air mitigation potential of urban vegetation (Baraldi et al., 2019; Contardo et al.,  
397 2020). Since there is sparse vegetation around the RU site (Fig. 1C), air pollution in this area reflects the high  
398 railway and road traffics and prevailing winds carrying air particles and soil dusts from one area to another.  
399

400 Cluster analysis (Fig. 2B) discriminated the more Eastern of the studied industrial sites, IZ4, in a single most  
401 dramatically contaminated Cluster 3. Indeed, compared to the traffic (e.g., roadside dust) and industrial (i.e.,  
402 pipes manufactures and gas processing) pollution determinants of the even more Eastern RU zone, atmospheric  
403 contamination at IZ4 may be amplified by emissions from a steel melting plant (EPE Rouiba Foundries) and  
404 would not benefit from the 'protective' effect of the RNR area discussed above. Multivariate analysis resulted in  
405 a common Cluster 2 for the other IZ1–3 industrial sites which can be considered having a similar poor air  
406 quality. Intriguingly, in Cluster 2 PLIs were found decreasing moving westward, i.e.,  $IZ1 \sim IZ3 < IZ2$  (Table 2),  
407 seemingly not associated to the prevalent dominant winds from the east in the region. Lastly, the TH control site  
408 considered as a relatively clean area, has been included in Group 4.

409 Arguably, the most probable common aerial elemental sources in IZ1–4 area could be vehicle emissions in  
410 the case of Ti, Cu, Sb, and Sn, and industrial activities for Al, Fe, Mn, and Cd (Bajpai and Upreti, 2012;  
411 Lucadamo et al., 2016; Ratier et al., 2018). This is consistent with CA and PCA calculations (Fig. 3B) indicating  
412 that highly bioaccumulable elements in lichens were found at IZ1–4 sites from several potential sources. The  
413 overall consistency between CA and PCA indexes may imply that the clustering of sample sites in the present  
414 study was done in a rather convincing pattern (Boamponsem et al., 2017).

#### 415 416 4.3. Trace element sources identification

417  
418 Both natural and anthropogenic emissions contribute locally to atmospheric trace elements enrichment and  
419 deposition. If grouping statistical methods permits establishing high correlations for particular elements in  
420 regional clusters to point out common specific local emitters (Boamponsem et al., 2010; Demiray et al., 2012),  
421 such identification is rather complex in practice because some of the elements can be emitted from several  
422 sources. Indeed, Cluster I elements discriminated by CA (Fig. 2C), mostly lithogenic (Agnan et al., 2015; Paoli  
423 et al., 2015), may also derive from anthropogenic sources such as road traffic, while the variability seen in  
424 Clusters II and III (this latter including Co, As, Th, Hf, Cs, Cr, Rb, Se, Sc, U, Sm, Eu, Yb, Lu, Tb, Hg, and In)  
425 mainly reflects noticeable anthropogenic industrial and agricultural activities.

426 PCA, a convenient statistical tool for exploring significant contamination sources in air, soil or water (Sorbo  
427 et al., 2008; Boamponsem et al., 2010; Zeng et al., 2015; Boonpeng et al., 2017), yielded a PC1 component (Fig.  
428 3A) predominantly correlated with 16 bioaccumulated elements (i.e., Cd, Cu, Cr, Pb, Ga, La, Ti, Ce, HF, Sm,  
429 Tb, Hg, Sb, V, U, and Th), being largely associated with industrial and vehicle emissions, and concentrating in  
430 the areas adjacent to high road traffic (Boamponsem et al., 2010; Aslan et al., 2013; Contardo et al., 2020). Some

431 elements from Clusters III (As, Sc, In, Rb, Cs, Lu) and I (Al, Fe, Mn, Zn) as well as Br were negatively  
432 correlated with the PC2 component and displayed high loadings, representing 16% of the total variance of the  
433 data set (Table S4; Supplementary materials). This factor could likely be constituted by a mixture of airborne  
434 elements arising from terrestrial, marine and industrial pollution (Incerti et al., 2017).

435

#### 436 4.4. *Assessing a general typology of air pollution in the Rouiba–Reghaia region*

437

438 The data of MCA analysis are discussed below for selected groups of contamination patterns defined in  
439 Figure 4.

440 The highest contamination score in Group 15 (CF4–EF5) reflects an extreme bioaccumulation of Sb and Ga  
441 in all IZ sites and RNR, respectively. MCA high score in Group 12 (CF4–EF4) indicated that these metals,  
442 together with Pb are also located at high levels ( $CF \geq 3$ ) in all industrial sites (except for Pb at IZ3), while Sb  
443 dominated in RU. The rise in Ga pollution seen here could be related to its increasing use in electronics  
444 manufacturing (arsenide and nitride derivatives are used in integrated circuits, optoelectronic devices,  
445 photodetectors, and solar cells) and nuclear medicine. However, still Ga environmental impact has not been  
446 adequately documented (White and Shine, 2016).

447 High concentrations of Sb and Pb found in this study are usually observed in the vicinity of oil refineries and  
448 chemical plants (Bajpai and Upreti, 2012; Lucadamo et al., 2016; Ratier et al., 2018). Also, these heavy metals  
449 are typically traffic-related pollutants, being emitted by fossil fuel combustion, tire and brake linings  
450 deterioration, vehicle component wearing, corrosion, lubricating oils or fuel additives (Lough et al., 2005;  
451 Fujiwara et al., 2011; Olowoyo et al., 2011; Gianini et al., 2012; Dong et al., 2017; Contardo et al., 2020;  
452 Parviainen et al., 2020). The high levels of Sb found in IZ sites and RU may originate from industrial sources  
453 metal melting and refining, waste combustion (Bergamaschi et al., 2004) or purification processes (Pacyna and  
454 Pacyna, 2001).

455 An earlier lichen biomonitoring survey of Pb contamination in the Algiers region, where the number of motor  
456 vehicles, often old and poorly maintained engines, has exceeded 1.4 million and current regulation for tetraethyl  
457 lead content allowance is as high as 0.6 g/L, identified road traffic as the main source of atmospheric Pb  
458 pollution (Rahali, 2002). Over the past two decades, this situation was getting worse in the Rouiba–Reghaia  
459 region where increased traffic congestion is contributing to an uncontrollable increase in Pb emissions (Bouhila  
460 et al., 2015) and it is noteworthy that Algeria was the last country to ban leaded gasoline in 2021. Therefore,



461 because elevated traffic-related atmospheric Pb emissions were still occurring at the time of the present study, it  
462 was speculated the substantial contamination levels shown in Table 1 would arise mostly from vehicular traffic.

463 For many years, the use of leaded gasoline in Europe was assumed as the main source for airborne Pb  
464 concentrations, making this metal a reliable indicator for road traffic-related airborne pollution (Zechmeister et  
465 al., 2005). In the 1990s, lead-free gasoline was made compulsory in European countries and many studies  
466 documented a significant decrease of airborne lead pollution (Loppi and Corsini, 2003; Loppi et al., 2004) and  
467 later investigations confirmed that Pb levels in lichens did not correlate anymore with any current road traffic  
468 (Paoli et al., 2013). Strikingly, Rola and Osyczka (2019) reported that despite the cessation of leaded fuel  
469 commercialization, lead still remains the most prevalent heavy metal in local urban environment likely due to its  
470 lengthy residence time and resuspension in roads and urban soils, but also in house dust and domestic heating  
471 systems (Loppi and Corsini, 2003; Levin et al., 2021). To sum up, *P. furfuracea* transplants, known to be  
472 particularly adapted as Pb biomonitors (Sorbo et al., 2008; Guidotti et al., 2009), may ideally report on possible  
473 changes in the atmosphere of Rouiba–Reghaia region consecutive to the current use of unleaded gasoline.

474 The pollution patterns of Group 17 (CF4–EF3) including Cd, Cu, Hg, and In imply these elements to arose  
475 predominantly from artificial sources. High accumulation was found in all monitoring sites for Cd, while Cu,  
476 Hg, and In were mostly seen in industrial sites, RNR, and IZ2,3, respectively. Despite its low crustal abundance  
477 Cd is widely used in industrial processes, e.g., phosphate fertilizers or anticorrosive agents for manufacturing Ni-  
478 Cd batteries. Other sources of Cd emissions include fossil fuels from traffic pollution, emissions from petroleum  
479 metallurgical facilities, electroplating, and polyvinyl chloride plastics (see, e.g., Scerbo et al., 2002).

480 In addition to typical sources of Hg pollution such as steel mills, cement plants, electronics and agrochemical  
481 industries (Scerbo et al., 2002; Demiray et al., 2012; Boonpeng et al., 2017), this gaseous and aerosol pollutant is  
482 known to be released from contaminated soils and water (López Berdonces et al., 2017; Perez Catán et al.,  
483 2020), presumably here in RNR by the polluted lake of Reghaia or the sea.

484 The anthropogenic origin of In contamination at IZ2,3 sites drawn from its high CFs (Table 2) is consistent  
485 with its use as tracer of melting and waste burning (Bruinen de Bruin et al., 2006) or in the production of LEDs  
486 and high-efficiency photovoltaic cells (White and Shine, 2016).

487 Last element of Group 17 examined, Cu, which exhibited extremely high CFs that increased by 7- to 10-fold  
488 in RU and IZ4 as compared to TH, respectively, is a typical contaminant (Boamponsem et al., 2010; Aslan et al.,  
489 2013; Contardo et al., 2020) associated to road traffic, agricultural practices (use of pesticides and fertilizers) or  
490 waste incineration, a common usage at Oued Smar landfill (only ~28 km away from IZ1 site; Fig. 1B). Lichens

491 biomonitoring is a particularly efficient technique for assessing urban Cu emissions (Vannini et al., 2019). The  
492 trends found here for Cu and other Group 17 elements are in accordance with recent reports in similar urban and  
493 industrial sites (see, e.g., Agnan et al., 2013).

494 In Group 14 (CF3–EF4), a high enrichment was found for Zn and Mn at IZ1 and RU, and for As at IZ2 and  
495 RU. Presumably, high contamination at IZ1 by Zn, a typical indicator for waste incineration, may have the same  
496 origin as that by Cu discussed above. In the urban area, Zn may also derive from motor vehicle traffic through  
497 the consumption of greasing oils (Boamponsem et al., 2017). Airborne Mn, an abundant and essential  
498 micronutrient used in fertilizers and manure, has been shown to induce neurotoxicity upon chronic inhalation of  
499 high doses (Kim et al., 2022). Last, bioaccumulation of As found in transplanted lichens appears consistent with  
500 known association to fuel combustion (Agnan et al., 2015), steelwork (Demiray et al., 2012), and areas of  
501 agriculture production (Pacyna and Pacyna, 2001; Zhou et al., 2018).

502 Among elements gathered in Group 16 (CF4–EF2), Lu, Th, and Yb were heavily accumulated but mildly  
503 enriched at all the IZ sites. Moreover, V, which was also found at RNR, is an environmental marker of vehicle  
504 exhaust (Giampaoli et al., 2016), being present in fuel oils, crude petroleum, coal, and is a common component  
505 of oil refinery catalysts (Adamo et al., 2003; Brunialti and Frati, 2007). As in Groups 17 and 14 discussed above,  
506 the infrastructures surrounding all studied sites, including RNR, may largely contribute to atmospheric metal  
507 pollution, a feature described in many other regions worldwide with high traffic and refinery activities  
508 (Enamorado-Báez et al., 2015; Zhao et al., 2019).

509 Conceivably, long distance emissions could contribute to even increase the intrinsic pollution within the  
510 Rouiba–Reghaia region. Among such potential ‘foreign’ metal emitters are the huge Sidi Rezine oil refinery, the  
511 Oued Smar industrial zone, and the Meftah cement factory. Also, frequent and strong southern Saharian winds in  
512 the region are natural carriers of main road (NR5,11, A1) dusts and rare earths.

513 Uptake of Al by lichens, which exhibited rare enrichment with low to medium contamination at RNR in  
514 Groups 2 (CF2–EF1) and 7 at IZ1,3 (CF3–EF1) sites, showed mild enrichment with heavy contamination in  
515 Group 16 at IZ2 (CF4–EF2). This element has a known mixed anthropogenic / natural origin (Agnan et al.,  
516 2015), e.g., it can accumulate in lichens due to the erosive action of the winds (Adamo et al., 2003) strongly  
517 blowing in the studied region or consecutive to airborne soils dust deposition (Paoli et al., 2015).

518 Of interest, high CFs and EFs were observed for Br in RNR (scoring at CF4–EF4 in Group 12) and TH sites.  
519 In addition to its known industrial uses (fire retardants, water treatments, dyes, pharmaceuticals, pesticides),  
520 bodies of water can represent major natural sources of Br (Bergamaschi, 2004).

521 Finally, while some heavy metals fortunately showed rather low (Fe, Rb, Sc, Sm, Co) or negligible (Ba) EFs  
522 and CFs, the scores for Cr and Ti indicated strong contamination but rare enrichment, suggesting a marginal  
523 contribution of anthropogenic emissions.

524

## 525 **5. Conclusions**

526 The findings in this study illustrate the accuracy of the information gained by biomonitoring methods  
527 combined to discriminant analysis of contaminated areas. To the authors' knowledge, this is the first  
528 comprehensive investigation (33 trace elements measured) of airborne metal pollution in Rouiba–Reghaia, one  
529 of the largest, most populated, and highly expanding urban–industrial and agricultural regions in Algeria. This  
530 was obtained by application of the transplant technique using the lichen *Pseudevernia furfuracea* which  
531 demonstrated outstanding accumulator properties, allowing detection of trace metal concentrations by XRF and  
532 INAA within only 3 months of exposure. Of the seven studied sites (comprising the unpolluted TH area) having  
533 quite different degrees of industrialization and urbanization the highest increases of atmospheric concentrations  
534 of toxic heavy metals (times with respect to TH) were: Cd (20–50), Cu (30–300), Pb (2–33), and Sb (5–80) and  
535 were found in those five distributed East–West along the NR5 and NR11 national roads, the Algiers–Blida  
536 railway, and the Houari Boumediene international airport. These elements and others (such as Ga, La, Cr, Cs, Ti,  
537 V, and Ce) were present in these zones at severe contamination levels (10–17 elements present at heavy  
538 contamination levels with  $CF > 3$ ) and found highly enriched at levels globally exceeding those reported in a  
539 number of comparable areas worldwide. Multivariate analysis scoring attempted to disentangle dominantly  
540 lithogenic (Al, Cr, Fe, Ti, Co, Rb, Sm, and Sc) vs. anthropogenic (e.g., Cd, Cu, Pb, Sb, V, and Zn) pollution  
541 sources, unsurprisingly tracing back to exploding human activity and vehicular density as key environmental  
542 causes. Expectedly, the finding that the wooded Reghaia Nature Reserve, located North-South with respect to the  
543 'pollution axis', behaved as a green barrier further highlights the high overall ecological risk in the  
544 Rouiba–Reghaia region, and the usefulness of establishing periodic registers of multi-elemental airborne  
545 contamination.

546

## 547 **Declaration of competing interest**

548 The authors declare they have no known competing financial interest or personal relationship that could have  
549 appeared to influence the work reported in this paper.  
550

551

553 **Credit author statement**

554  
555 **Henia Saib:** Conceptualization, Methodology, Investigation, Data curation, Writing - original draft. **Amine**  
556 **Yekkour:** Formal analysis. **Mohamed Toumi:** Resources. **Bouzid Guedioura:** Investigation, Data  
557 curation. **Mohamed Amine Benamar:** Resources. **Abdelhamid Zeghdaoui:** Investigation. **Annabelle**  
558 **Austruy:** Methodology, Resources. **David Bergé-Lefranc:** Formal analysis, Methodology. **Marcel**  
559 **Culcasi:** Formal analysis, Writing – review & editing, Visualization. **Sylvia Pietri:** Conceptualization,  
560 Project administration, Supervision, Funding acquisition, Writing – review & editing.

561  
562 **Acknowledgements**

563 Authors thank the Agence Nationale de la Recherche (ANR MitoDiaPM – N° ANR-17-CE34-0006-01), the  
564 CNRS (Centre National de la Recherche Scientifique) and the French Higher Education and Research Ministry  
565 for funding part of this study. Authors wish to thank people at SIG office (for the conception and realization of  
566 the database) and at BNEDER (National Study Office for Rural Development) for contribution to the  
567 implementation of the map of study area. H.S. gratefully thanks people at NUR Research Reactor and Physics  
568 and Nuclear Application Division/CRND (Draria, Algeria) for experimental support, especially with irradiation  
569 procedures. Ms. L. Diaz (University of Pau, France) is gratefully acknowledged for her valuable contribution to  
570 this paper.  
571

572  
573 **Appendix A. Supplementary materials:** Supplementary data to this article can be found online.

574  
575 **Figure captions**

576  
577 **Figure 1.** (A) General map of the Rouiba–Reghaia region (Eastern of Algiers) showing the unpolluted Theniet  
578 El-Had area (TH). (B) Enlargment showing the location of the main eighteen sampling sites (\*) in the industrial-  
579 urbanized region. (C) Typologies of the six studied areas (RU, RNR, and IZ1–4; gray backgrounds) as obtained  
580 by cluster analysis of trace elements contents (see Fig. 2A). Arabic numbers refer to the sampling site  
581 coordinates presented in Table S1.

582  
583 **Figure 2.** Dendrograms obtained by cluster analysis of (A) the 21 sampling sites, (B) the seven studied areas,  
584 and (C) the 33 monitored elements. Arabic (1–4) and roman (I–III) numerals refer to Clusters of sites and groups  
585 of elements, respectively. Cluster analysis was performed from the measured metal concentrations in lichens in  
586 the six monitoring sites as compared to the unpolluted TH area (in red).

587  
588 **Figure 3.** Principal component analysis biplot (PC1 vs. PC2) of elements in lichens at the each monitoring site.  
589 A) Loading vectors of elements. B) Elements were symbolized according to the three main Clusters I (**▲**), II (**□**),  
590 and III (**○**) resulting from cluster analysis of Fig. 2C and monitoring sites plot. Pollution load index (PLI; black  
591 arrow) is also plotted as a supplementary variable.

592  
593 **Figure 4.** Multiple correspondence analysis biplot (MC1 vs. MC2) of elements and their corresponding classes  
594 of contamination factor (CF)–enrichment factor (EF) at monitoring sites The considered classes were: CF1 (CF  
595 class 1):  $CF < 1.2$ , no contamination; CF2 (CF class 2):  $1.2 \leq CF < 2$ , light contamination; CF3 (CF class 3):  $2 \leq$   
596  $CF < 3$ , medium contamination; CF4 (CF class 4):  $CF \geq 3$ , heavy contamination; EF class 1 (EF1):  $EF \leq 1$ , rarely  
597 enriched (soil and crust source); EF class 2 (EF2):  $1 < EF \leq 10$ , mildly enriched (natural and artificial sources);  
598 EF class 3 (EF3):  $10 < EF \leq 100$ , moderately enriched (artificial sources); EF class 4 (EF4):  $100 < EF \leq 1000$ ,  
599 highly enriched; EF class 5 (EF5):  $EF > 1000$ , extremely enriched. Numerals with boldface (1–17) refer to  
600 chemical elements monitored in the considered sites (indicated between hooks) that obtained similar MCA  
601 plotting scores as follow: 1 (CF1–EF1): Ba [IZ1–4, IZ3, RU, RNR], Co [RU], Fe [IZ2, RU, RNR], Lu [RU], Rb  
602 [IZ2, RNR], Sc [IZ4, RNR], Yb [RNR]; 2 (CF2–EF1): Al [RNR], Co [IZ1, IZ3,4], Fe [IZ3], Nd [IZ4], Rb  
603 [IZ1,3], Sc [RU], Sm [RU]; 3 (CF1–EF4): Br [IZ1,3], Sb [RNR], Se [RNR, RU, IZ1,2]; 4 (CF2–EF4): Sb  
604 [RNR]; 5 (CF1–EF2): As [IZ1,3,4], Br [RU, IZ4], Cs [IZ3], Eu [RU], Mn [IZ3], In [RU, IZ4]; 6 (CF1–EF3): Se  
605 [IZ3,4], Zn [IZ3]; 7 (CF3–EF1): Al [IZ1,3], Co [IZ2], Fe [IZ4], V [RU], Yb [RU]; 8 (CF2–EF2): Co [RNR], Nd  
606 [RNR, RU, IZ1], Tb [RNR], U [RU]; 9 (CF4–EF1): Cr [RNR, RU, IZ1–4], Sc [IZ2], Sm [IZ2,4], Tb [IZ4], Ti  
607 [RNR, RU, IZ2–4], U [IZ4], V [IZ2]; 10 (CF2–EF3): As [RNR], Mn [RNR], Zn [RNR], In [RNR, IZ1]; Hg  
608 [RU, IZ1–4]; 11 (CF3–EF4): Br [IZ2], Pb [RNR]; 12 (CF4–EF4): Br [RNR], Ga [RU, IZ1–4], Pb [RU, IZ1,2,4],  
609 Sb [RU]; 13 (CF3–EF2): Al [RU], Eu [IZ1, IZ2], Fe [IZ1], Hf [RU, IZ3], Lu [RNR], Mn [IZ4], Nd [IZ2,3], Sm  
610 [RNR, IZ1,3], Th [RNR, RU], U [RNR, IZ3]; 14 (CF3–EF4): As [RU, IZ2], Hf [RNR], Mn [RU, IZ1], Zn  
611 [RU, IZ1]; 15 (CF4–EF5): Ga [RNR], Sb [IZ1–4]; 16 (CF4–EF2): Al [IZ2, IZ4], Ce [RU, IZ2–4], Cs [IZ2,4], Cu  
612 [RNR, RU], Eu [IZ3,4], Hf [IZ2,4], La [RNR, RU], Lu [IZ1–4], Mn [IZ2], Rb [RU, IZ4], Sc [IZ1, IZ3], Tb [RU,  
613 IZ1–3], Th [IZ1–4], Ti [IZ1], U [IZ1,2], V [RNR, IZ1,3,4], Yb [IZ1–4]; 17 (CF4–EF3): Cd [RNR, RU, IZ1–4],  
614 Ce [RNR, IZ1], Cs [RNR, RU, IZ1], Cu [IZ1–4], Eu [RNR], Hf [IZ1], Hg [RNR], In [IZ2,3], La [IZ1–4], Pb  
615 [IZ3], Zn [IZ2,4].

**Table 1**

Elements concentrations<sup>a</sup> ( $\mu\text{g}\cdot\text{g}^{-1}$  dw) in thalli of transplanted lichens<sup>b</sup> *Pseudevernia furfuracea* v. *furfuracea* in the control (TH) and urban-industrial monitoring sites<sup>c</sup>.

Element	TH		RNR		RU		IZ1		IZ2		IZ3		IZ4	
	Mean	Min–Max	Mean	Min–Max	Mean	Min–Max	Mean	Min–Max	Mean	Min–Max	Mean	Min–Max	Mean	Min–Max
Al	573	548–603	921**	909–930	1539***	1482–1611	1168**	987–1270	2640***	2480–2840	1588***	1524–1690	4396***	4328–4470
As	0.33	0.32–0.35	0.66**	0.53–0.79	0.98	0.69–1.45	0.24	0.22–0.26	0.66	0.64–0.68	0.24	0.19–0.33	0.25	0.25–0.26
Ba	6.20	5.30–6.70	1.28***	1.27–1.30	1.61***	1.22–2.13	2.70***	2.41–2.85	4.47**	4.21–4.85	2.62***	2.30–2.80	5.68	5.52–5.80
Br	17.5	15.5–18.9	5.4***	4.8–6.1	3.2***	2.2–4.1	18.0	16.4–19.5	37.8***	36.5–38.9	15.0	12.0–17.0	3.2***	3.1–3.2
Cd	0.21	0.16–0.25	4.90**	3.85–6.25	4.20*	3.50–5.30	6.30**	5.70–7.20	5.80**	4.90–7.00	4.30**	4.10–4.50	31.30***	29.4–34.5
Co	0.23	0.20–0.28	0.45	0.22–0.72	0.25	0.22–0.32	0.31	0.25–0.38	0.57**	0.50–0.62	0.31	0.28–0.35	0.39	0.37–0.43
Cu	0.2	0.2–0.3	6.0	5.31–7.01	41.2**	29.9–59.3	39.3*	25.9–57.4	41.6**	38.9–45.3	39.6**	29.4–55.8	59.0**	45–75
Cr	0.07	0.07–0.08	1.02**	0.98–1.05	1.29**	0.96–1.59	1.41***	1.25–1.52	1.67***	1.56–1.82	1.50***	1.37–1.60	1.73***	1.58–1.89
Cs	0.15	0.15–0.16	0.65***	0.52–0.76	0.88***	0.79–0.99	0.64***	0.61–0.68	0.96***	0.90–1.02	0.14	0.14–0.15	1.56***	1.51–1.60
In	0.05	0.05–0.06	0.07	0.07–0.08	0.05	0.05–0.06	0.10**	0.09–0.11	0.30***	0.27–0.35	0.36***	0.30–0.41	0.05	0.05–0.06
Fe	1031	1006–1050	670**	620–675	484***	390–573	2598***	2580–2614	986	887–1059	1968***	1940–2010	2561***	2356–2752
Ga	0.6	0.6–0.7	50.0***	49.0–51.0	20.6**	15.8–25.8	10.9	9.2–11.9	33.0***	30.0–36.0	12.0	10.8–12.7	59.5***	47–72
Hf	0.19	0.17–0.22	0.56***	0.54–0.57	0.53***	0.49–0.57	0.65***	0.61–0.72	0.79***	0.76–0.85	0.49**	0.42–0.55	0.88***	0.76–0.98
La	0.72	0.71–0.75	2.50	1.72–3.80	5.40	3.86–7.93	50.03**	29.7–67.8	33.60*	22.5–44.7	46.4**	33.2–66.1	71.4***	59.7–85
Ce	1.3	0.3–1.9	7.6**	6.3–9.4	10.4**	8.5–12.8	9.7**	8.7–10.4	10.9***	9.7–11.8	8.28**	6.7–9.4	12.5***	9.8–16
Nd	0.98	0.92–1.05	1.52	1.50–1.58	1.27	1.28–1.43	1.20	1.18–1.23	2.28**	1.73–2.95	2.28**	1.98–2.54	1.96*	1.40–2.54
Sm	0.08	0.06–0.09	0.18**	0.17–0.19	0.14	0.08–0.19	0.21**	0.17–0.25	0.24***	0.22–0.26	0.19**	0.18–0.21	0.27***	0.25–0.28
Eu	0.05	0.01–0.07	0.25	0.24–0.26	0.06	0.03–0.07	0.14	0.09–0.21	0.13	0.09–0.15	0.35*	0.09–0.53	0.75***	0.65–0.85
Tb	0.01	0.01–0.02	0.02	0.01–0.02	0.06*	0.05–0.07	0.07*	0.05–0.07	0.13***	0.09–0.18	0.06*	0.05–0.07	0.06*	0.05–0.07
Yb	0.05	0.04–0.06	0.04	0.03–0.05	0.04	0.03–0.04	0.15	0.07–0.24	0.16	0.08–0.25	0.17	0.09–0.27	0.47*	0.44–0.50
Lu	0.01	0.01–0.02	0.05	0.02–0.08	0.01	0.01–0.02	0.07*	0.06–0.07	0.08**	0.05–0.09	0.08*	0.05–0.14	0.08*	0.06–0.09
Mn	79	60–92	119**	111–125	173**	111–254	228**	220–235	250***	240–260	53	49–60	181**	167–201
Hg	0.03	0.03–0.04	0.09**	0.08–0.09	0.04	0.03–0.04	0.05*	0.02–0.08	0.06**	0.05–0.07	0.06**	0.04–0.09	0.06**	0.03–0.08
Rb	0.11	0.09–0.13	0.09	0.09–0.10	9.43***	9.10–9.82	0.21**	0.19–0.21	0.09	0.09–0.10	0.17***	0.17–0.18	9.40***	8.23–10.65
Sb	0.25	0.21–0.30	0.32	0.28–0.35	1.30	0.97–1.55	7.95	2.60–12.85	12.03**	5.59–17.95	15.89**	11.80–20.10	20.00***	18.5–21.7

**Table 1 (continued)**

Sc	0.10	0.10–0.11	0.12	0.11–0.13	0.18**	0.15–0.21	0.43***	0.39–0.46	0.37***	0.35–0.39	0.84***	0.83–0.85	0.06	0.06–0.06 Se
1.02	0.99–1.05	0.13***	0.12–0.14	0.13***	0.12–0.13	0.12***	0.11–0.13	0.31***		0.30–0.32	0.15*	0.13–0.17	0.13*	0.11–0.15 Pb
8.0	6.5–9.5	19.0	17.0–20.0	31.1	25.0–37.9	202**	119–266	162**		136–190	253***	181–321	268***	198–350 Ti
0.2	0.1–0.2	18.5	16.3–21.1	53.9**	45.7–66.3	103.0***	92.0–115.0	134.0***		115–154	98.6***	89–109	73***	69–80
V	0.71	0.66–0.81	6.46	3.22–9.61	1.68	1.02–2.71	5.99***	2.05–9.21	3.14**	2.84–3.58	4.12***	1.70–6.96	11.86***	7.68–15.32
Th	0.12	0.11–0.13	0.28	0.28–0.29	0.27	0.26–0.29	0.50*	0.40–0.60	0.51**	0.43–0.61	0.79***	0.66–0.98	0.81***	0.71–0.91 U
0.04	0.03–0.04	0.09**	0.05–0.12	0.06	0.05–0.07	0.14	0.07–0.18	0.13***		0.11–0.17	0.12	0.07–0.17	0.15***	0.15–0.16 Zn
37	29–42	67	61–71	75*	70–83	78**	68–93	114***		98–124	44.	27–59	113***	93–128

<sup>a</sup>Values expressed as means  $\pm$  standard deviation from three independent determinations performed in duplicate, were obtained by INAA, except for Pb and Cd which were measured by XRF. <sup>b</sup>Transplanted lichens were exposed for 3 months during the winter period (January–April). <sup>c</sup>TH, Thniet El-Had; RNR, Reghaia nature reserve; RU, Reghaia urban site; IZ1–4, Rouiba–Reghaia industrial zones. Significance (ANOVA followed by Dunnett's test) vs. values at TH site: \* $P < 0.5$ , \*\* $P < 0.01$ , and \*\*\* $P < 0.001$ .

**Table 2**

Contamination factor (CF), enrichment factor (EF), and pollution load index (PLI) calculated<sup>a</sup> from the trace elements concentrations accumulated in the transplanted lichens *Pseudevernia furfurcea* at study sites<sup>b</sup>.

Element	RNR		RU		IZ1		IZ2		IZ3		IZ4	
	CF	EF	CF	EF	CF	EF	CF	EF	CF	EF	CF	EF
Al	1.6	0.8	2.7	1.6	2.0	0.3	4.6	1.8	2.7	0.6	7.6	1.7
As	1.9	32.8	2.9	22.7	0.7	9.3	2.0	11.4	0.7	4.1	0.7	2.7
Ba	0.2	0.3	0.2	0.2	0.4	0.5	0.7	0.3	0.4	0.3	0.9	0.3
Br	12.0	203	0.2	67	1.0	531	2.2	493	0.9	325	0.2	24.7
Cd	23.0	22.5	19.7	15.0	29.5	29.9	27.2	12.2	20.2	15.0	147	39.4
Co	1.9	1.6	1.1	0.5	1.3	0.9	2.5	0.7	1.3	0.6	1.7	0.3
Cu	28	5.3	187	3.7	179	50.3	189	21.5	180	34.3	270	18.5
Cr	14.5	0.9	18.2	0.7	19.9	1.0	23.6	0.5	21.0	0.8	24.3	0.3
Cs	4.2	19.4	5.7	15.8	4.2	15.0	6.3	10.0	0.5	1.2	10.1	9.7
In	1.4	26.6	1.0	5.4	1.9	29.6	6.0	38.3	7.2	75.5	1.0	1.9
Fe	0.6	1.0	0.5	0.5	2.5	3.2	1.0	0.5	1.9	0.8	2.4	0.9
Ga	79	2347	32	578	17	405	52	543	19	328	94	588
Hf	2.9	16.6	2.8	9.5	3.4	15.4	4.1	8.2	2.5	8.5	4.6	5.5
La	3.4	5.7	7.4	7.4	68.9	90.5	46.2	26.9	63.9	61.8	98.3	34.3
Ce	5.8	10.2	8.0	8.3	7.4	10.2	8.3	5.1	6.3	6.4	9.6	3.5
Nd	1.5	3.3	1.2	1.6	1.2	2.0	2.3	1.7	2.3	2.8	2.0	0.8
Sm	2.2	2.3	1.7	1.0	2.6	2.1	3.0	1.0	2.4	1.5	3.3	0.7
Eu	4.9	11.3	1.1	1.5	2.7	4.9	2.4	2.0	6.9	9.2	14.6	7.0
Tb	1.5	1.6	4.6	2.9	4.8	4.0	9.0	3.3	4.5	2.7	4.5	1.0
Yb	0.6	0.8	2.6	0.5	3.0	3.3	3.2	1.6	3.3	2.7	9.3	2.7
Lu	2.8	3.7	0.7	0.9	4.1	6.5	4.4	3.0	4.9	5.6	4.5	1.9
Mn	1.5	11.8	2.1	10.2	2.8	17.0	3.1	8.6	0.7	3.0	2.3	3.7
Hg	3.0	99.8	1.3	18.8	1.6	48.0	1.8	24.0	1.9	46.0	1.8	13.6



**Table 2 (continued)**

Rb	0.7	1.0	85.7	6.1	1.9	0.2	0.9	0.4	1.5	0.1	85.6	2.1
Sc	1.2	0.5	1.8	0.5	4.1	1.3	3.6	0.5	8.2	2.0	0.6	0.1
Se	0.1	238.3	0.1	137.5	0.1	171.9	0.3	196.2	0.2	93.8	0.1	47.9
Pb	2.4	118	3.9	119	25.3	102	20.2	361	31.6	93	33.5	359
Ti	123	0.3	359	0.6	686	1.3	893	0.7	653	0.9	486	0.2
V	9.0	5.0	2.4	0.8	8.4	3.7	4.4	0.8	5.8	1.9	16.7	1.9
Th	2.3	2.6	2.3	1.5	4.2	3.7	4.3	1.7	6.5	4.3	6.8	1.6
U	2.3	3.1	1.7	1.3	3.4	3.6	3.3	1.6	2.8	2.2	3.8	1.0
Zn	1.8	84.9	2.0	60.0	2.1	78.5	3.0	50.8	1.1	32.6	3.0	30.4
<b>PLI index</b>	2.87		3.18		4.68		5.86		4.61		7.08	

<sup>a</sup> CF, EF and PLI indexes were calculated as indicated in the methods section. For each element at the TH control site, CF, EF and PLI values of 1 are taken as the background level. Ranges of CF, EF and PLI values were respectively categorized into the following contamination classes:

CF indicator:  $CF < 1.2$ , no contamination,  $1.2 \leq CF < 2$ , light contamination,  $2 \leq CF < 3$ , medium contamination, and  $CF \geq 3$ , heavy contamination.

EF indicator:  $EF \leq 1$ , rarely enriched (soil and crust source);  $1 < EF \leq 10$ , mildly enriched (natural and artificial sources);  $10 < EF \leq 100$ , moderately enriched (artificial sources);  $100 < EF \leq 1000$ , highly enriched;  $EF > 1000$ , extremely enriched.

PLI indicator:  $PLI < 0.9$ , no pollution;  $1 \pm 0.1$ , background level;  $1.1 < PLI < 1.5$ , low pollution;  $1.5 \leq PLI < 2.0$ , moderate pollution;  $2.0 \leq PLI < 2.5$ , high pollution;  $PLI \geq 2.5$ , very high pollution.

<sup>b</sup> RNR, Reghaia nature reserve; RU, Reghaia urban site; IZ1–4, Rouiba–Reghaia industrial zones.

**Table 3**

Elements concentrations ( $\mu\text{g}\cdot\text{g}^{-1}\text{dw}$ ) in thalli of various lichens transplanted in several industrial and urban sites worldwide.

<b>Element</b>	This work, Algeria <sup>a</sup>	Sao Paulo, Brazil <sup>b</sup>	Jesi, Italy <sup>c</sup>	Sarajevo, Bosnia Herzegovina <sup>d</sup>	Netherlands <sup>e</sup>	Naples, Italy <sup>f</sup>	Genoa, Italy <sup>g</sup>	Fos-sur-Mer, France <sup>h</sup>	Hebei, China <sup>i</sup>
Al	2042 ± 1219	7129 ± 137	628 ± 89.5	—	5800 (230–21000)	1969	820±120	3661±1554	8971 (3561–14024)
As	0.5 ± 0.32	1.057 ± 14	0.35 ± 0.03	1.76 ± 0.08	5.7 (0.5–17)	0.60	—	2.39 ± 1.12	—
Ba	3.06 ± 1.6	—	12.2 ± 1.42	28.6 ± 1.2	—	—	21.9 ± 6.5	—	82.9 (42.7–186.7)
Br	13.76 ± 12.5	24.85 ± 0.05	—	10 ± 0.4	56 (15–170)	—	—	—	—
Cd	9.46 ± 10	3917 ± 209	0.12 ± 0.01	0.53 ± 0.08	2.8 (0.6–21)	1.36	0.12 ± 0.01	0.48 ± 0.24	1.43 (0.83–2.3)
Co	0.38 ± 0.1	1063 ± 4	0.29 ± 0.11	0.62 ± 0.03	2 (0.2–6.3)	2.76	0.54 ± 0.09	1.24 ± 0.42	1.81 (1.31–2.89)
Cu	37.87 ± 19	—	10.5 ± 2.04	> 6	33 (1.4–120)	29.6	38 ± 53	17.9 ± 11.1	14.73 (8.36–32.3)
Cr	1.4 ± 0.2	16.4 ± 0.1	1.88 ± 0.36	8.32 ± 0.33	26 (4–270)	4.49	6.4 ± 0.9	30.0 ± 16.6	—
Cs	0.75 ± 0.4	1016 ± 10	0.08 ± 0.01	0.45 ± 0.02	0.8 (0.2–5)	—	—	—	1.89 (1.17–2.81)
In	0.14 ± 0.1	—	—	> 0.2	—	—	—	—	—
Fe	1544 ± 897	4135 ± 21	575 ± 49.9	1630 ± 65	5800 (720–30000)	1423	820 ± 220	14.11 ± 11.78	6542 (3446–10146)
Ga	31 ± 19	—	0.17 ± 0.03	0.74 ± 0.08	47 (2.3–180)	—	—	—	—
Hf	0.65 ± 0.15	1464 ± 5	—	0.258 ± 0.01	1.4 (0.09–8)	—	—	—	—
La	34.9 ± 2.7	7.05 ± 0.05	—	1.4 ± 0.06	6.2 (0.8–35)	—	—	—	19.06 (13.1–33.3)
Ce	9.9 ± 2.1	16.58 ± 0.04	—	3.02 ± 0.16	—	—	—	—	—
Nd	1.75 ± 0.50	—	—	1.35 ± 0.07	—	—	—	—	—
Sm	0.20 ± 0.05	1055 ± 1	—	0.3 ± 0.01	—	—	—	—	2.4 (1.76–3.94)
Eu	0.27 ± 0.2	181 ± 2	—	0.060 ± 0.006	—	—	—	—	—
Tb	0.067 ± 0.03	103 ± 3	—	0.037 ± 0.002	—	—	—	—	0.30 (0.20–0.46)
Yb	0.17 ± 0.16	346.6 ± 6.7	—	0.122 ± 0.006	0.4 (0.078–3)	—	—	—	—
Lu	0.064 ± 0.03	60.1 ± 0.5	—	—	0.071 (0.001–0.46)	—	—	—	—

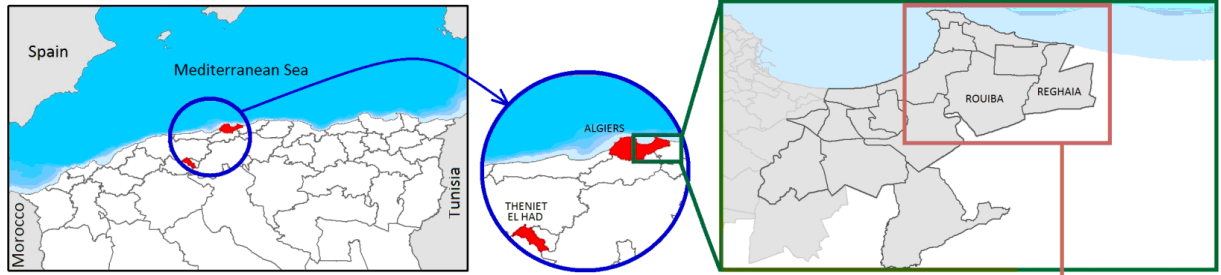
**Table 3 (continued)**

Mn	167 ± 72	164.4 ± 1.2	51.1 ± 6.52	—	110 (16–400)	64.5	84 ± 27	194±116.7	124.5 (59.4–242.4)
Hg	0.062 ± 0.02	—	—	—	0.5 (0.1–36)	—	—	—	—
Rb	4.40 ± 3.9	20.2 ± 0.2	3.27 ± 0.66	7.71 ± 0.31	13 (1.8–62)	—	—	—	17.72 (11.35–24.34)
Sb	9.59 ± 8	2000 ± 10	—	0.5 ± 0.03	3.3 (0.3–12)	—	—	1.71 ± 0.61	1 (0.64–2.17)
Sc	0.33 ± 0.26	1190 ± 3	—	0.52 ± 0.03	1.1 (0.16–5.2)	—	—	—	—
Se	0.163 ± 0.07	665 ± 24	0.37 ± 0.38	0.169 ± 0.012	1.8 (0.4–7.5)	—	—	—	—
Pb	155.95 ± 111	—	4.91 ± 0.98	—	150 (3.1–370)	152	5.9 ± 3.2	21.4 ± 9.4	172.8 (55.3–271.1)
Ti	80.18 ± 39	510 ± 89	0.01 ± 0.00	—	—	39.07	—	—	433.2 (272–614)
V	5.54 ± 4	190.2 ± 8.7	1.71 ± 0.15	—	32 (5.7–99)	5.41	3 ± 1.2	11.7 ± 4.4	17.08 (9.35– 26)
Th	0.53 ± 0.2	—	—	0.41 ± 0.02	1.2 (0.14–8.9)	—	—	—	2.37 (1.14–3.41)
U	0.118 ± 0.03	—	0.19 ± 0.02	0.145 ± 0.007	0.57 (0.09–2.7)	—	—	—	—
Zn	81.9 ± 28.0	145.7 ± 0.5	40.8 ± 33.2	88.9 ± 3.6	210 (61–1100)	243.3	69 ± 19	70.9 ± 49.6	121.2 (61–241.3)

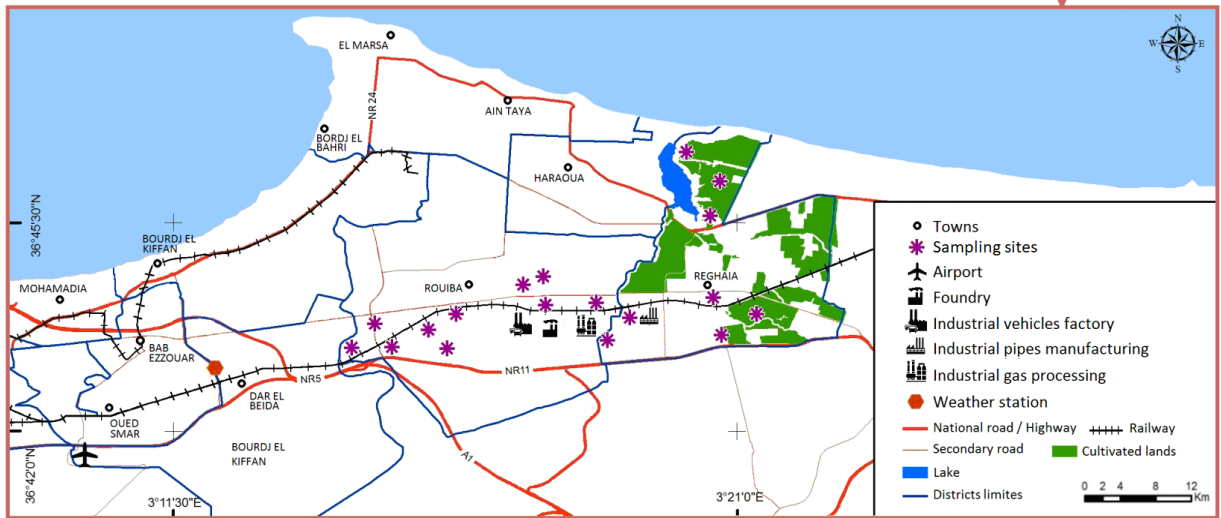
<sup>a</sup>*Pseudevernia furfuracea* (L.) Zopf, transplanted for 3 months during the winter season in the Rouiba–Reghaia region. For each element, data are expressed as the average of 3 independent values (means ± standard deviation) recorded in the 6 monitoring sites of the Rouiba–Reghaia region (RNR, RU and IZ1–4). <sup>b</sup>*Canoparmelia texana* (Saiki et al., 1997). <sup>c</sup>*Evernia prunastri*, transplanted for three months (Fрати et al., 2005). <sup>d</sup>*Hypogymnia physodes* sampled in situ (Humerovic et al., 2015). <sup>e</sup>*Parmelia sulcata*, sampled in situ (de Bruin, 1990). <sup>f</sup>*Pseudevernia furfuracea* transplanted for four months (Adamo et al., 2003). <sup>g</sup>*Pseudevernia furfuracea* transplanted for one month (Malaspina et al., 2014). <sup>h</sup>*Xanthoria parietina* in situ (Ratier et al., 2018). <sup>i</sup>*Rhizoplaca chrysoleuca* transplanted for twelve months (Zhao et al., 2019).

**FIGURE 1**

**A**



**B**



**C**

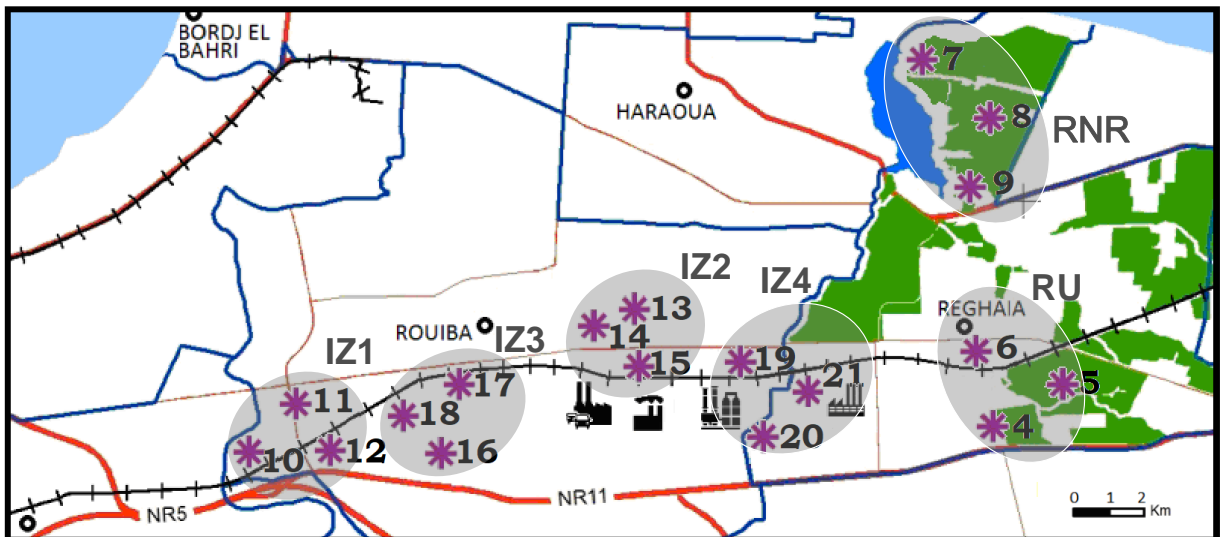


**FIGURE 2**

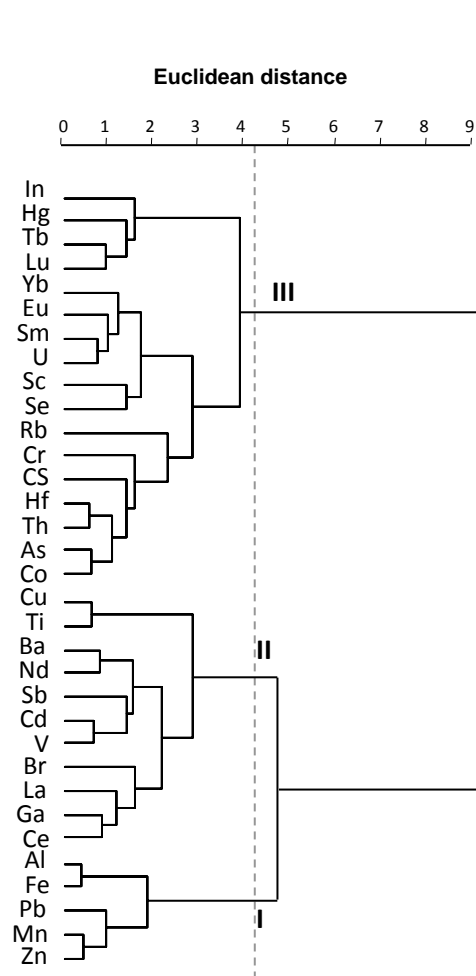
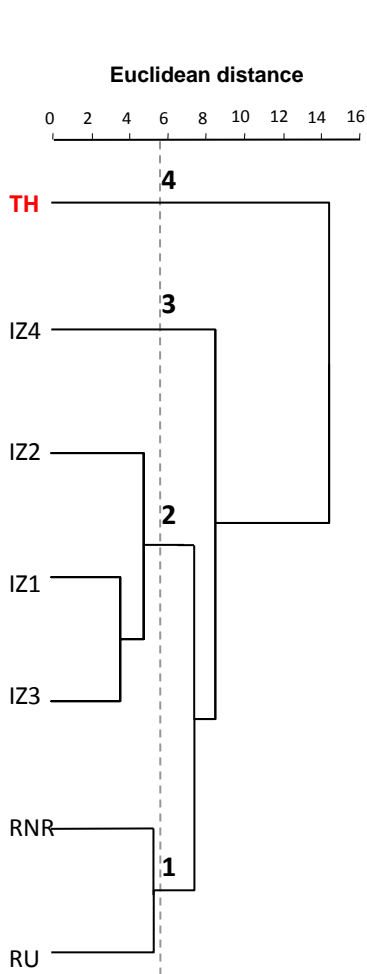
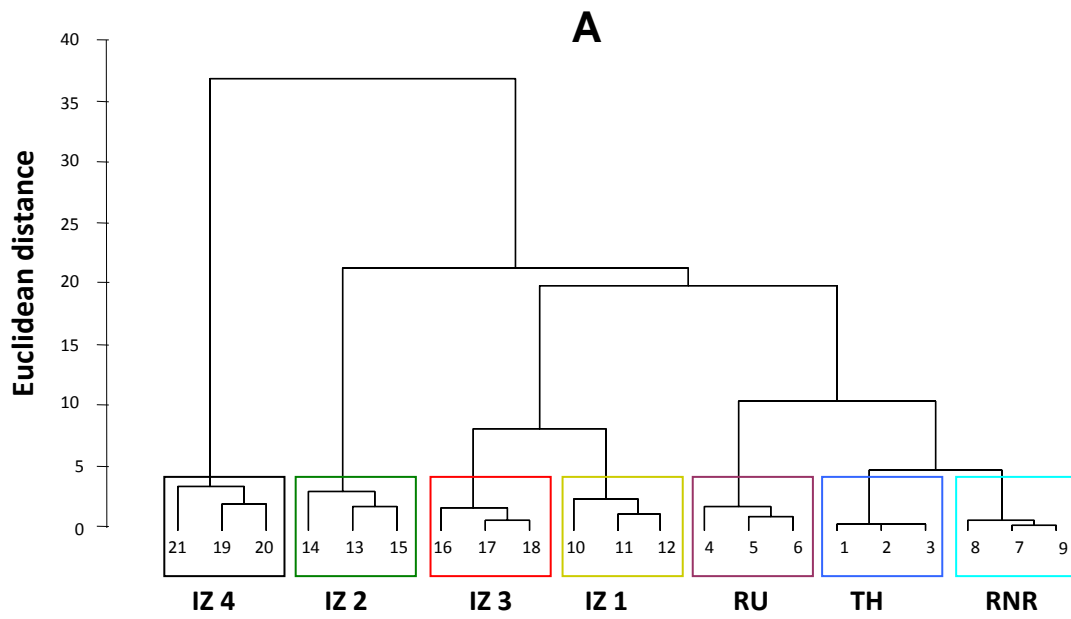


**FIGURE 3**

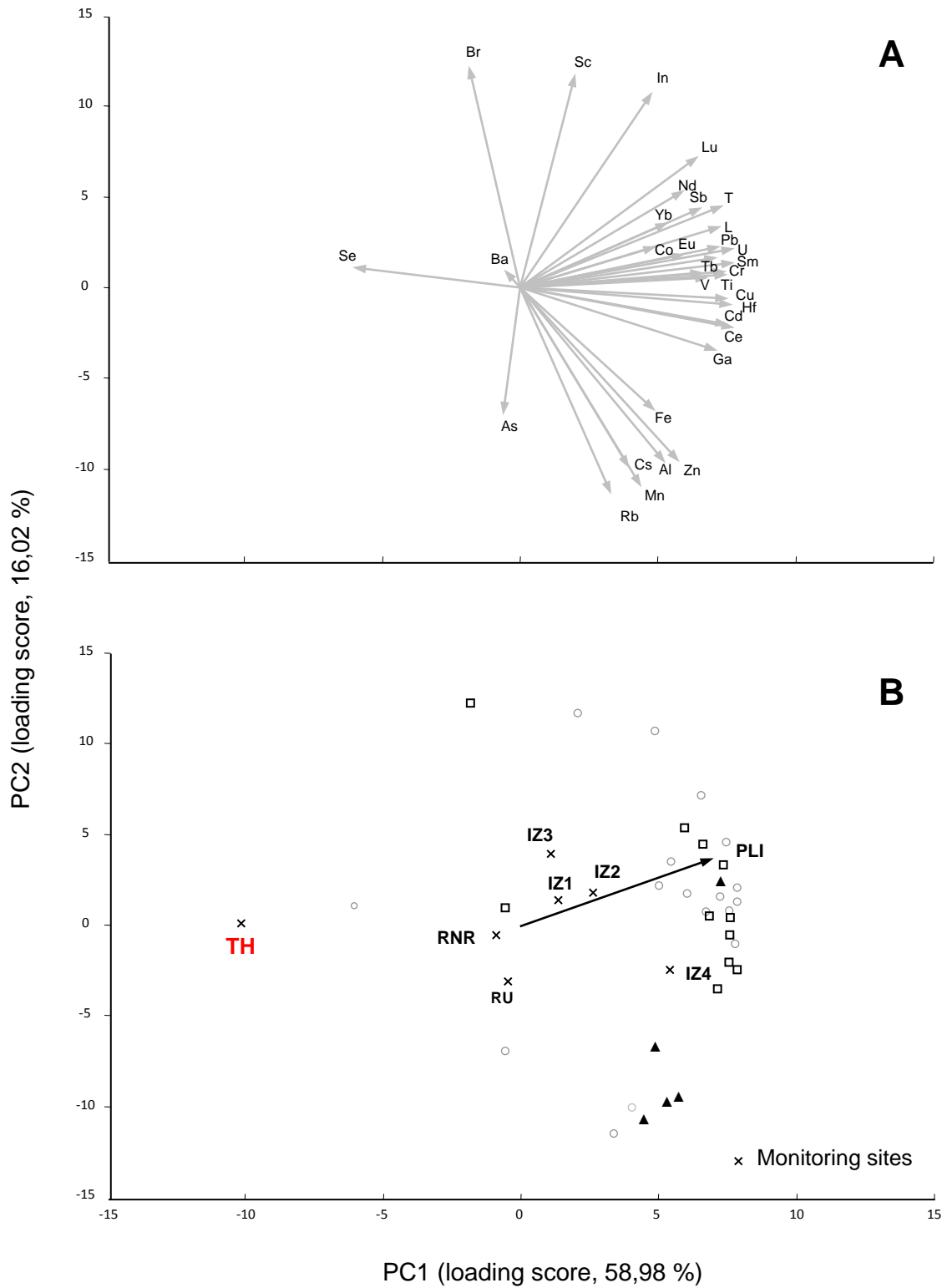
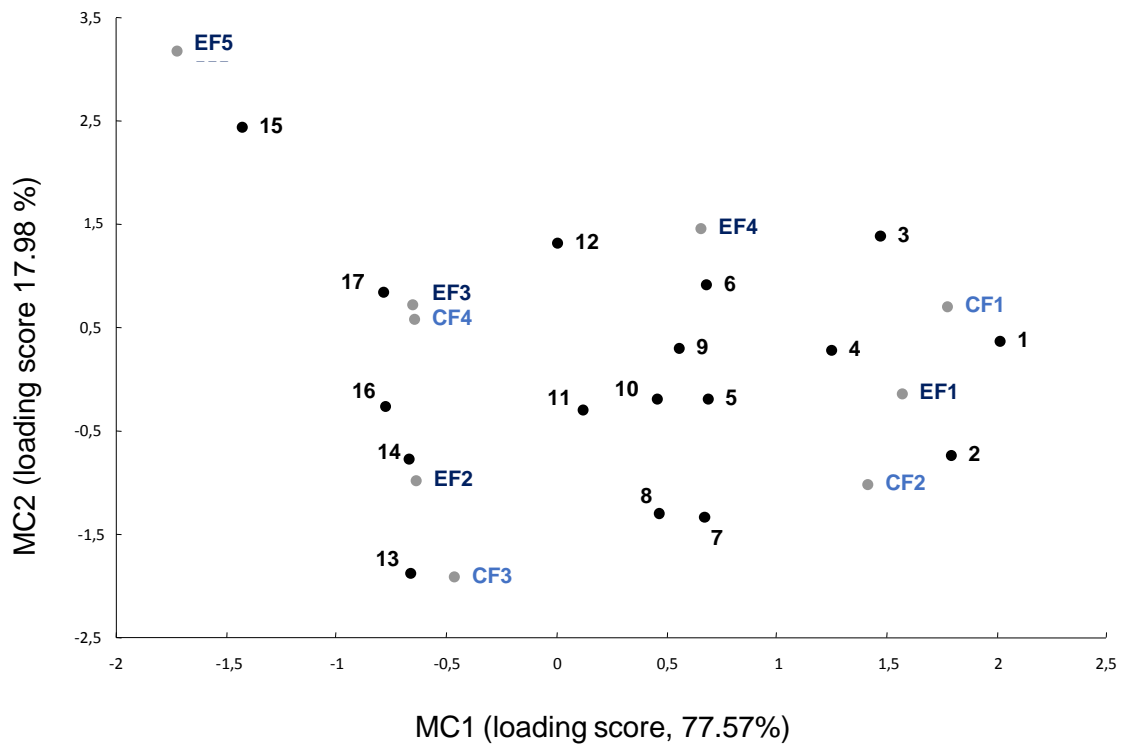


**FIGURE 4**



## References

- Adamo, P., Giordano, S., Vingiani, S., Castaldo Cobiانchi, R., Violante, P., 2003. Trace element accumulation by moss and lichen exposed in bags in the city of Naples (Italy). *Environ. Pollut.* 122, 91–103. [https://doi.org/10.1016/S0269-7491\(02\)00277-4](https://doi.org/10.1016/S0269-7491(02)00277-4)
- Agnan, Y., Séjalon-Delmas, N., Probst, A., 2013. Comparing early twentieth century and present-day atmospheric pollution in SW France: A story of lichens. *Environ. Pollut.* 172, 139–148. <https://doi.org/10.1016/j.envpol.2012.09.008>
- Agnan, Y., Séjalon-Delmas, N., Claustres, A., Probst, A., 2015. Investigation of spatial and temporal metal atmospheric deposition in France through lichen and moss bioaccumulation over one century. *Sci. Total Environ.* 529, 285–296. <https://doi.org/10.1016/j.scitotenv.2015.05.083>
- Agnan, Y., Séjalon-Delmas, N., Probst, A., 2017. Evaluation of lichen species resistance to atmospheric metal pollution by coupling diversity and bioaccumulation approaches: A new bioindication scale for French forested areas. *Ecol. Indic.* 72, 99–110. <http://dx.doi.org/10.1016/j.ecolind.2016.08.006>
- Adjiri, F., Ramdani, M., Iograda, T., Chalard, P., 2018. Bio-monitoring of metal trace elements by epiphytic lichen in the Bordj BouArreridj area, east of Algeria. *Der Pharma Chem.* 10(3), 1–8.
- Ancora, S., Dei, R., Rota E., Mariotti, G., Bianchi, N., Bargagli, R., 2021. Altitudinal variation of trace elements deposition in forest ecosystems along the NW side of Mt. Amiata (central Italy): Evidence from topsoil, mosses and epiphytic lichens. *Atmos. Pollut. Res.* 12, 101200. <https://doi.org/10.1016/j.apr.2021.101200>
- Aslan, A., Gurbuz, H., Yazici, K., Cicek, A., Turan, M., Ercisli, S., 2013. Evaluation of lichens as bio-indicators of metal pollution. *J. Elem.* 18, 353–369. <http://dx.doi.org/10.5601/jelem.2013.18.3.01>
- Austruy, A., Yung, L., Ambrosi, J.P., Girardclos, O., Keller, C., Angeletti, B., Dron, J., Chamaret, P., Chalot, M., 2019. Evaluation of historical atmospheric pollution in an industrial area by dendrochemical approaches. *Chemosphere* 220, 116–126. <https://doi.org/10.1016/j.chemosphere.2018.12.072>
- Bajpai, R., Upreti, D., 2012. Accumulation and toxic effect of arsenic and other heavy metals in a contaminated area of West Bengal, India, in the lichen *Pyxine cocolos* (Sw.). *Nyl. Ecotox. Environ. Safe.* 83, 63–70. <https://doi.org/10.1016/j.ecoenv.2012.06.001>
- Baraldi, R., Chieco, C., Neri, L., Facini, O., Rapparini, F., Morrone, L., Carriero, G., 2019. An integrated study on air mitigation potential of urban vegetation: from a multi-trait approach to modeling. *Urban For. Urban Green.* 41, 127–138. <https://doi.org/10.1016/j.ufug.2019.03.020>
- Bari, A., Rosso, A., Minciardi, M.R., Troiani, F., Piervittori, R., 2001. Analysis of heavy metals in atmospheric particulates in relation to their bioaccumulation in explanted *Pseudevernia furfuracea* thalli. *Environ. Monit. Assess.* 69, 205–220. <https://doi.org/10.1023/A:1010757924363>
- Basile, A., Sorbo, S., Aprile, G.G., Conte, B., Castaldo Cobiانchi, R., 2008. Comparison of the heavy metal bioaccumulation capacity of an epiphytic moss and an epiphytic lichen. *Environ. Pollut.* 151, 401–407. <https://doi.org/10.1016/j.envpol.2007.07.004>
- Bergamaschi, L., Rizzio, E., Giaveri, G., Profumo, A., Loppi, S., Gallorini, M., 2004. Determination of baseline element composition of lichens using samples from high elevations. *Chemosphere* 55, 933–939. <https://doi.org/10.1016/j.chemosphere.2003.12.010>
- Boamponsem, L.K., Adam, J.I., Dampare, S.B., Nyarko, B.J.B., Essumang, D.K., 2010. Assessment of atmospheric heavy metal deposition in the Tarkwa gold mining area of Ghana using epiphytic lichens. *Nucl. Instrum. Methods Phys. Res. B* 268, 1492–1501. <https://doi.org/10.1016/j.nimb.2010.01.007>
- Boamponsem, L.K., De Freitas, C.R., Williams, D., 2017. Source apportionment of air pollutants in the Greater Auckland Region of New Zealand using receptor models and elemental levels in the lichen, *Parmotrema reticulatum*. *Atmos. Pollut. Res.* 8, 101–113. <https://doi.org/10.1016/j.apr.2016.07.012>
- Boonpeng, C., Polyiam, W., Sriviboon, C., Sangiamdee, D., Watthana, S., Nimis, P., Boonpragob, K., 2017. Airborne trace elements near a petrochemical industrial complex in Thailand assessed by the lichen *Parmotrema tinctorum* (Despr. ex Nyl.) Hale. *Environ. Sci. Pollut. Res.* 24, 12393–12404. <https://doi.org/10.1007/s11356-017-8893-9>
- Bouhila, Z., Mouzai, M., Azli, T., Nedjar, A., Mazouzi, C., Zergoug, Z., Boukhadra, D., Chegrouche, S., Lounici, H., 2015. Investigation of aerosol trace element concentrations nearby Algiers for environmental



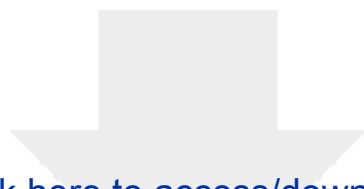
- monitoring using instrumental neutron activation analysis. *Atmos. Res.* 166, 49–59.  
<https://doi.org/10.1016/j.atmosres.2015.06.013>
- Bozkurt, Z., 2017. Determination of airborne trace elements in an urban area using lichens as biomonitor. *Environ. Monit. Assess.* 189, 573. <https://doi.org/10.1007/s10661-017-6275-x>
- Brunialti, G., Frati, L., 2007. Biomonitoring of nine elements by the lichen *Xanthoria parietina* in Adriatic Italy: A retrospective study over a 7-year time span. *Sci. Total Environ.* 387, 289–300.  
<https://doi.org/10.1016/j.scitotenv.2007.06.033>
- Contardo, T., Vannini, A., Sharma, K., Giordani, P., Loppi, S., 2020. Disentangling sources of trace element air pollution in complex urban areas by lichen biomonitoring. A case study in Milan (Italy). *Chemosphere.* 256, 127155. <https://doi.org/10.1016/j.chemosphere.2020.127155>
- Conti, M.E., Cecchetti, G., 2001. Biological monitoring: lichens as bioindicators of air pollution assessment - a review. *Environ. Pollut.* 114, 471–492. [https://doi.org/10.1016/S0269-7491\(00\)00224-4](https://doi.org/10.1016/S0269-7491(00)00224-4)
- Culicov, O.A., Yurukova, L.D., 2006. Comparison of element accumulation of different moss- and lichen-bags, exposed in the city of Sofia (Bulgaria). *J. Atmos. Chem.* 55, 1–12. <https://doi.org/10.1007/s10874-005-9002-x>
- Cuny, D., Van Haluwyn, C., Pesch, R., 2001. Biomonitoring of trace elements in air and soil compartments along the motorway in France. *Water Air Soil Pollut.* 125, 273–289. <https://doi.org/10.1023/A:1005278900969>
- de Bruin, M., 1990. Applying biological monitors and neutron activation analysis in studies of heavy-metal air pollution. Moss, tree bark, lichens and other materials can yield important information about environmental pollution and its likely sources. *IAEA Bull.* 4, 22–27.
- Bruinen de Bruin, Y., Koistinen, K., Yli-Tuomi, T., Kephelopoulos, S., Jantunen, M., 2006. A review of source apportionment techniques and marker substances available for identification of personal exposure, indoor and outdoor sources of chemicals. Joint Research Centre Institute for Health and Consumer Protection, Publication Office of the European Commission, Directorate General, EUR 22349EN.
- Demiray, A.D., Yolcubal, I., Akyol, N.H., Cobanoglu, G., 2012. Biomonitoring of airborne metals using the lichen *Xanthoria parietina* in Kocaeli Province, Turkey. *Ecol. Indic.* 18, 632–643.  
<https://doi.org/10.1016/j.ecolind.2012.01.024>
- Demková, L., Baranová, B., Oboňa, J., Árvay, J., Lošák, T., 2017. Assessment of air pollution by toxic elements on petrol stations using moss and lichen bag technique. *Plant Soil Environ.* 8, 355–361.  
<https://doi.org/10.17221/297/2017-PSE>
- Dong, S., Gonzalez, R.O., Harrison, R.M., Green, D., North, R., Fowler, G., Weiss, D., 2017. Isotopic signatures suggest important contributions from recycled gasoline, road dust and non-exhaust traffic sources for copper, zinc and lead in PM10 in London, United Kingdom. *Atmos. Environ.* 165, 88–98.  
<https://doi.org/10.1016/j.atmosenv.2017.06.020>
- Dron, J., Ratier, A., Austruy, A., Revenko, G., Chaspoul, F., Wafo, E., 2021. Effect of meteorological conditions and topography on the bioaccumulation of PAHs and metal elements by native lichen (*Xanthoria parietina*). *J. Environ. Sci.* 109, 193–205. <https://doi.org/10.1016/j.jes.2021.03.045>
- Enamorado-Báez, S.M., Gómez-Guzmán, J.M., Chamizo, E., Abril, J.M., 2015. Levels of 25 trace elements in high-volume air filter samples from Seville (2001–2002): Sources, enrichment factors and temporal variations. *Atmos. Res.* 155, 118–129. <http://dx.doi.org/10.1016/j.atmosres.2014.12.005>
- Filzmoser, P., Reimann, C. 2002. Robust Multivariate Methods in Geostatistics. In: Gaul, W., Ritter, G. (eds) *Classification, Automation, and New Media. Studies in Classification, Data Analysis, and Knowledge Organization.* Springer, Berlin, Heidelberg. [https://doi.org/10.1007/978-3-642-55991-4\\_46](https://doi.org/10.1007/978-3-642-55991-4_46)
- Frati, L., Brunialti, G., Loppi, S., 2005. Problems related to lichen transplants to monitor trace element deposition in repeated surveys: a case study from central Italy. *J. Atmos. Chem.* 52, 221–230.  
<https://doi.org/10.1007/s10874-005-3483-5>
- Freitas, M.C., Catarino, F.M., Branquinho, C., Maguas, C., 1993. Preparation of a lichen reference material. *J. Radioanal. Nucl. Chem.* 169, 47–55. <https://doi.org/10.1007/BF02046782>
- Fujiwara, F., Rebagliati, R.J., Marrero, J., Gomez, D., Smichowski, P., 2011. Antimony as a traffic-related element in size-fractionated road dust samples collected in Buenos Aires. *Microchem. J.* 97, 62–67.  
<https://doi.org/10.1016/j.microc.2010.05.006>

- Gallo, L., Corapi, A., Loppi, S., Lucadamo, L., 2014. Element concentrations in the lichen *Pseudevernia furfuracea* (L.) Zopf transplanted around a cement factory (S Italy). *Ecol. Indic.* 46, 566–574. <https://doi.org/10.1016/j.ecolind.2014.07.029>
- Garty, J., Weissman, L., Tamir, O., Beer, S., Cohen, Y., Karnieli, A., Orlovsky, L., 2000. Comparison of five physiological parameters to assess the vitality of the lichen *Ramalina lacera* exposed to air pollution. *Physiol. Plant.* 109(4), 410–418. <https://doi.org/10.1034/j.1399-3054.2000.100407.x>
- Giampaoli, P., Wannaz, E.D., Tavares, A.R., Domingos, M., 2016. Suitability of *Tillandsia usneoides* and *Aechmea fasciata* for biomonitoring toxic elements under tropical seasonal climate. *Chemosphere* 149, 14–23. <https://doi.org/10.1016/j.chemosphere.2016.01.080>
- Gianini, M., Fischer, A., Gehrig, R., Ulrich, A., Wichser, A., Piot, C., Hueglin, C., 2012. Comparative source apportionment of PM10 in Switzerland for 2008/2009 and 1998/1999 by positive matrix factorisation. *Atmos. Environ.* 54, 149–158. <https://doi.org/10.1016/j.atmosenv.2012.02.036>
- Greenacre, M., 2017. Correspondence analysis in practice. Third Edition. Interdisciplinary Statistics Series. Chapman & Hall/CRC, New York. <https://doi.org/10.1201/9781315369983>
- Guedioura, B., Bendjaballah, N., Alioui, N., 2014. Profiling measurements of metal ion distribution in thin polymer inclusion membranes by Rutherford backscattering spectrometry. *Radiat. Eff. Defects Solids* 169, 388–395. <https://doi.org/10.1080/10420150.2013.865621>
- Guidotti, M., Stella, D., Dominici, C., Blasi, G., Owczarek, M., Vitali, M., Protano, C., 2009. Monitoring of traffic-related pollution in a province of central Italy with transplanted lichen *Pseudevernia furfuracea*. *Bull. Environ. Contam. Toxicol.* 83, 852–858. <https://doi.org/10.1007/s00128-009-9792-7>
- Herrero Fernández, Z., Estevez Álvarez, J. R., Montero Álvarez, A., Pupo González, I., dos Santos Júnior, J.A., Ortueta Milan, M., Padilla Álvarez, R., 2015. Multielement analysis of lichen samples using XRF methods. Comparison with ICP-AES and FAAS. *Xray Spectrom.* 45, 77–84. <https://doi.org/10.1002/xrs.2657>
- Humerovic, J., Muhic-Sarac, T., Memic, M., Zero, S., Selovic, A., 2015. Multielement and rare earth element composition of the soil and lichen from Sarajevo, Bosnia and Herzegovina. *Ekolozi* 24, 36–44. <http://dx.doi.org/10.5053/ekolozi.2015.10>
- Incerti, G., Cecconi, E., Capozzi, F., Adamo, P., Bargagli, R., Benesperi, R., Carniel, F.C., Cristofolini, F.S., Giordano, S., Puntillo, D., Spagnuolo, V., Tretiach, M., 2017. Intraspecific variability in baseline element composition of the epiphytic lichen *Pseudevernia furfuracea* in remote areas: implications for biomonitoring of air pollution. *Environ. Sci. Pollut. Res.* 24, 8004–8016. <https://doi.org/10.1007/s11356-017-8486-7>
- Kim, H., Harrison F.E., Aschner, M., Bowman, A.B., 2022. Exposing the role of metals in neurological disorders: a focus on manganese. *Trends. Mol. Med.* 28, 555–568. <https://doi.org/10.1016/j.molmed.2022.04.011>
- Kłós, A., Rajfur, M., Waclawek, M., 2011. Application of enrichment factor (EF) to the interpretation of results from the biomonitoring studies. *Ecol. Chem. Eng.* S18, 171–183. <https://doi.org/10.1016/j.molmed.2022.04.011>
- Kodnik, D., Winkler, A., Carniel, F.C., Tretiach, M., 2017. Biomagnetic monitoring and element content of lichen transplants in a mixed land use area of NE Italy. *Sci. Total Environ.* 595, 858–867. <https://doi.org/10.1016/j.scitotenv.2017.03.261>
- Lê, S., Josse, J., Husson, F., 2008. FactoMineR: An R package for multivariate analysis. *J. Stat. Softw.* 25, 1–18. <https://doi.org/10.18637/jss.v025.i01>
- Legendre, P., Legendre, L., 1998. *Numerical Ecology*. Second Edition, Elsevier Science Ltd., Amsterdam.
- Levin, R., Zilli Vieira, C.L., Rosenbaum, M.H., Bischoff, K., Mordarski, D.C., Brown, M.J., 2021. The urban lead (Pb) burden in humans, animals and the natural environment. *Environ. Res.* 193, 110377. <https://doi.org/10.1016/j.envres.2020.110377>
- Lide, D.R., (Ed.), 2005. *CRC Handbook of Chemistry and Physics, Section 14: Geophysics, Astronomy and Acoustics; Abundance of Elements in the Earth's Crust and in the Sea 85th Ed.*, CRC Press, Boca Raton, FL, USA.
- López Berdonces, M.A., Higuera, P.L., Fernández-Pascual, M., Borreguero, A.M., Carmona, M., 2017. The role of native lichens in the biomonitoring of gaseous mercury at contaminated sites. *J. Environ. Manage.* 15, 186, 207–213. <https://doi.org/10.1016/j.jenvman.2016.04.047>

- Loppi, S., Corsini, A., 2003, 'Diversity of epiphytic lichens and metal contents of *Parmelia caperata* thalli as monitors of air pollution in the town of Pistoia'. *Environ. Monit. Assess.* 86, 289–301. <https://doi.org/10.1023/A:1024017118462>
- Loppi, S., Frati, L., Paoli, L., Bigagli, V., Rossetti, C., Bruscoli, C., Corsini, A., 2004. Biodiversity of epiphytic lichens and heavy metal contents of *Flavoparmelia caperata* thalli as indicators of temporal variations of air pollution in the town of Montecatini Terme (central Italy). *Sci. Total Environ.* 326, 113-122. <https://doi.org/10.1016/j.scitotenv.2003.12.003>
- Lough, G.C., Schauer, J.J., Park, J.S., Shafer, M.M., DeMinter, J.T., Weinstein, J.P., 2005. Emissions of metals associated with motor vehicle roadways. *Environ. Sci. Technol.* 39, 826–836. <https://doi.org/10.1021/es048715f>
- Lucadamo, L., Corapi, A., Loppi, S., De Rosa, R., Barca, D., Vespasiano, G., Gallo, L., 2016. Spatial variation in the accumulation of elements in thalli of the lichen *Pseudevernia furfuracea* (L.) Zopf transplanted around a biomass power plant in Italy. *Arch. Environ. Contam. Toxicol.* 70, 506–521. <https://doi.org/10.1007/s00244-015-0238-4>
- Lucadamo, L., Gallo, L., Corapi, A., 2022. Detection of air quality improvement within a suburban district (southern Italy) by means of lichen biomonitoring. *Atmos. Pollut. Res.* 13, 101346. <https://doi.org/10.1016/j.apr.2022.101346>
- Maatoug, M., Medkour, K., Ait Hammou, M., Ayad, N., 2010. Cartography of atmospheric pollution by the lead from road traffic using transplantation of a lichen bioaccumulator *Xanthoria parietina* in Tiaret city (Algeria). *Pollut. Atmos.* 205, 93–101. <http://dx.doi.org/10.4267/pollution-atmospherique.734>
- Malaspina, P., Giordania, P., Modenesi, P., Abelmoschi, M.L., Magi, E., Soggia, F., 2014. Bioaccumulation capacity of two chemical varieties of the lichen *Pseudevernia furfuracea*. *Ecol. Indic.* 45, 605–610. <https://doi.org/10.1016/j.ecolind.2014.05.026>
- Massimi, L., Conti, M.E., Mele, G., Ristorini, M., Astolfi, M.L., Canepari, S., 2019. Lichen transplants as indicators of atmospheric element concentrations: a high spatial resolution comparison with PM10 samples in a polluted area (Central Italy). *Ecol. Indic.* 101, 759–769. <https://doi.org/10.1016/j.ecolind.2018.12.051>
- Nannoni, F., Santolini, R., Protano, G., 2015. Heavy element accumulation in *Evernia prunastri* lichen transplants around a municipal solid waste landfill in central Italy. *Waste Manage.* 43, 353–362. <https://doi.org/10.1016/j.wasman.2015.06.013>
- Olowoyo, J., van Heerden, E., Fischer, J.L., 2011. Trace element concentrations from lichen transplants in Pretoria, South Africa. *Environ. Sci. Pollut. Res.* 18, 663–668. <https://doi.org/10.1007/s11356-010-0410-3>
- Osyczka, P., Boroń, P., Lenart-Boroń, A., Rola, K., 2018. Modifications in the structure of the lichen *Cladonia* thallus in the aftermath of habitat contamination and implications for its heavy-metal accumulation capacity. *Environ. Sci. Pollut. Res.* 25, 1950–1961. <https://doi.org/10.1007/s11356-017-0639-1>
- Pacheco, A.M.G., Freitas, M.C., 2009. Trace-element enrichment in epiphytic lichens and tree bark at Pico Island, Azores, Portugal. *J. Air Waste Manage. Assoc.* 59, 411-418. <https://doi.org/10.3155/1047-3289.59.4.411>
- Pacyna, J.M., Pacyna, E.G., 2001. An assessment of global and regional emissions of trace metals to the atmosphere from anthropogenic sources worldwide. *Environ. Rev.* 9, 269–298. <https://doi.org/10.1139/a01-012>
- Pantelica, A., Cercasov, V., Steinnes, E., Bode, P., Wolterbeek, H., 2016. Determination of 54 elements in lichen transplants: Comparison of INAA, ICPMS, and EDXRF. *Rom. J. Phys.* 61, 1380–1388.
- Paoli, L., Munzi, S., Fiorini, E., Gaggi, C., Loppi, S., 2013. Influence of angular exposure and proximity to vehicular traffic on the diversity of epiphytic lichens and the bioaccumulation of traffic-related elements. *Environ. Sci. Pollut. Res.* 20, 250-259. <https://doi.org/10.1007/s11356-012-0893-1>
- Parviainen, A., Papanlioti, E. M., Casares-Porcel, M., Garrido, C. J., 2020. Antimony as a tracer of non-exhaust traffic emissions in air pollution in Granada (S Spain) using lichen bioindicators. *Environ. Pollut.* 263, 114482. <https://doi.org/10.1016/j.envpol.2020.114482>
- Paoli, L., Munzi, S., Guttová, A., Senko, D., Sardella, G., Loppi, S., 2015. Lichens as suitable indicators of the biological effects of atmospheric pollutants around a municipal solid waste incinerator (S Italy). *Ecol. Indic.* 52, 362–370. <https://doi.org/10.1016/j.ecolind.2014.12.018>

- Perez Catán, S., Bubach, D., Messuti, M.I., Arribére, M.A., Guevara, S.R. 2020. Mercury in a geothermal and volcanic area in Patagonia, southern South America. *Atmos. Pollut. Res.* 11, 566–573. <https://doi.org/10.1016/j.apr.2019.12.005>
- Rahali, M., 2002. Mapping of lead pollution in Algiers area with a lichen (*Xanthoria parietina*) as indicator. *Pollut. Atmos.* 175, 421–432. <http://dx.doi.org/10.4267/pollution-atmospherique.2605>
- Ratier, A., Dron, J., Revenko, G., Austruy, A., Dauphin, C.E., Chaspoul, F., Wafo, E., 2018. Characterization of atmospheric emission sources in lichen from metal and organic contaminant patterns. *Environ. Sci. Pollut. Res.* 25, 8364–8376. <https://doi.org/10.1007/s11356-017-1173-x>
- Rehman, K., Fatima, F., Waheed, I., Hamid Akach, M.S., 2018. Prevalence of exposure of heavy metals and their impact on health consequences. *J. Cell. Biochem.* 119, 157–184. <https://doi.org/10.1002/jcb.26234>
- Rekik, B., Derbal, M., Lebbou, K., Benammar, M.E.A., 2016. Yb<sup>3+</sup>-doped LiBi (WO<sub>4</sub>)<sub>2</sub> single crystals fibers grown by micro-pulling down technique and characterization. *J. Cryst. Growth* 452, 101–104. <http://dx.doi.org/10.1016%2Fj.jcrysgro.2016.03.022>
- Reiman, C., Decarital, P., 2000. Intrinsic flaws of element enrichment factors (Efs) in environmental geochemistry. *Environ. Sci. Technol.* 34, 5084–5091. <https://doi.org/10.1021/es001339o>
- Rola, K., Osyczka, P., 2019. Temporal changes in accumulation of trace metals in vegetative and generative parts of *Xanthoria parietina* lichen thalli and their implications for biomonitoring studies. *Ecol. Indic.* 96, 293–302. <https://doi.org/10.1016/j.ecolind.2018.09.004>
- Saiki, M., Chaparro, C.G., Vasconcellos, M.B.A., Marcelli, M.P., 1997. Determination of trace elements in lichens by instrumental neutron activation analysis. *J. Radioanal. Nucl. Chem.* 217, 111–115. <https://doi.org/10.1007/BF02055358>
- Scerbo, R., Ristori, T., Possentin, L., Lampugnani, L., Barale, R., Barghigiani, C., 2002. Lichen (*Xanthoria parietina*) biomonitoring of trace element contamination and air quality assessment in Pisa Province (Tuscany, Italy). *Sci. Total Environ.* 286, 27–40. [https://doi.org/10.1016/s0048-9697\(01\)00959-7](https://doi.org/10.1016/s0048-9697(01)00959-7)
- Semadi, A., 1994. Lead pollution monitoring by transplanted lichens in Annaba area (Algeria). *Pollut. Atmos.* 140, 86–102.
- Sorbo, S., Aprile, G., Strumia, S., Castaldo Cobiانchi, R., Leoned, A., Basile, A., 2008. Trace element accumulation in *Pseudevernia furfuracea* (L.) Zopf exposed in Italy's so-called Triangle of Death. *Sci. Total Environ.* 407, 647–654. <https://doi.org/10.1016/j.scitotenv.2008.07.071>
- Swanton, C., Hill, W., Lim, E., Lee, C., Weeden, C.E., Augustine, M., Chen, K., Kuan, F.C., Marongiu, F., Rodrigues, F., Cha, H., Jacks, T., Luchtenborg, M., Malanchi, I., Downward, J., Carlsten, C., Hackshaw, A., Litchfield, K.R., DeGregori, J., Jamal-Hanjani, M. 2022. Mechanism of action and an actionable inflammatory axis for air pollution induced non-small cell lung cancer: Towards molecular cancer prevention. *Ann. Oncol.* 33 Supp. 7, S1413. <https://doi.org/10.1016/j.annonc.2022.08.046>
- Vannini, A., Paoli, L., Russo, A., Loppi, S., 2019. Contribution of submicronic (PM<sub>1</sub>) and coarse (PM<sub>>1</sub>) particulate matter deposition to the heavy metal load of lichens transplanted along a busy road. *Chemosphere* 231, 121–125. <https://doi.org/10.1016/j.chemosphere.2019.05.085>
- Vuković, G., Urošević, M.A., Škrivanj, S., Milićević, T., Dimitrijević, D., Tomašević, M., Popović, A., 2016. Moss bag biomonitoring of airborne toxic element decrease on a small scale: A street study in Belgrade, Serbia. *Sci. Total Environ.* 542, 394–403. <https://doi.org/10.1016/j.scitotenv.2015.10.091>
- White, S.J.O., Shine, J.P., 2016. Exposure potential and health impacts of indium and gallium, metals critical to emerging electronics and energy technologies. *Curr. Environ. Health Rep.* 3, 459–467. <https://doi.org/10.1007/s40572-016-0118-8>
- Wu, Y.Y., Gao, J., Zhang, G.Z., Zhao, R.K., Liu, A.Q., Sun L.W., Li, X., Tang, H.L., Zhao, L.C., Guo, X.P., Liu, H.J., 2020. Two lichens differing in element concentrations have similar spatial patterns of element concentrations responding to road traffic and soil input. *Sci. Rep.* 10, 19001. <https://doi.org/10.1038/s41598-020-76099-x>
- Xiong, Q., Zhao, W., Zhao, J., Zhao, W., Jiang, L., 2017. Concentration levels, pollution characteristics and potential ecological risk of dust heavy metals in the metropolitan area of Beijing, China. *Int. J. Environ. Res. Public Health* 14, 1159. <https://doi.org/10.3390/ijerph14101159>

- Zechmeister, H.G., Hohenwallner, D., Riss, A., Hanus-Ilmar, A., 2005. Estimation of element deposition derived from road traffic sources by using mosses. *Environmental Pollution* 138, 238–249. <https://doi.org/10.1016/j.envpol.2005.04.005>
- Zeng, X., Liu, Y., You, S., Zeng, G., Tan, X., Hu, X., Huang, L., Li, F., 2015. Spatial distribution, health risk assessment and statistical source identification of the trace elements in surface water from the Xiangjiang river, China. *Environ. Sci. Pollut. Res.* 22, 9400–9412. <https://doi.org/10.1007/s11356-014-4064-4>
- Zhao, L., Zhang, C., Jia, S., Liu, Q., Chen, Q., Li, X., Liu, X., Wu, Q., Zhao, L., Liu, H., 2019. Element bioaccumulation in lichens transplanted along two roads: The source and integration time of elements. *Ecol. Indic.* 99, 101–110. <https://doi.org/10.1016/j.ecolind.2018.12.020>
- Zhou, Y. Niu, L., Liu, K., Yin, S., Liu W., 2018. Arsenic in agricultural soils across China: Distribution pattern, accumulation trend, influencing factors, and risk assessment. *Sci. Total Environ.* 616–617, 156–163. <https://doi.org/10.1016/j.scitotenv.2017.10.232>



Click here to access/download

**e-Component**

Revised Supplementary materials.docx

